*Wiley Interdisciplinary Reviews: Climate Change*

WILEY

WIREs CLIMATE CHANGE

ADVANCED REVIEW

# El Niño Southern Oscillation Reconstructions During the Last Millennium

Mandy B. Freund[1,2,3] | Danielle C. Verdon-Kidd[4] | Kathryn J. Allen[5] | Josephine R. Brown[1,3]

[1]School of Geography, Earth and Atmospheric Sciences, University of Melbourne, Parkville, Victoria, Australia | [2]CSIRO Environment, Melbourne, Australia | [3]ARC Centre of Excellence for the Weather of the 21st Century, University of Melbourne, Parkville, Victoria, Australia | [4]School of Environmental and Life Sciences, University of Newcastle, Newcastle, New South Wales, Australia | [5]School of Geography, Planning, and Spatial Sciences, University of Tasmania, Hobart, Tasmania, Australia

**Correspondence:** Mandy B. Freund (mandy.freund@unimelb.edu.au)

**Received:** 2 September 2024 | **Revised:** 13 November 2025 | **Accepted:** 16 November 2025

**Editor-in-Chief:** Daniel Friess | **Domain Editor:** Eduardo Zorita

**Keywords:** El Niño | ENSO | La Niña | palaeoclimate | proxy | reconstructions

## ABSTRACT

The El Niño/Southern Oscillation (ENSO) constitutes the largest single source of interannual climate variability on a global scale, yet our understanding of its characteristics is limited by a focus on the modern instrumental era. To study ENSO characteristics during the pre-industrial era we rely on reconstructions of ENSO developed from a range of environmental proxies, documentary sources and palaeoclimate model simulations. Here we review the ENSO reconstructions from a range of sources covering the last millennium to assess characteristics of interannual ENSO variability and examine evidence for changes in ENSO characteristics over time. Despite differences in target variables (i.e., ENSO indices, seasonal window) and record durations, several reconstructions show broadly similar patterns, including periods of reduced ENSO variability in the mid 14th century, mid 18th and 19th centuries, whereas high variance periods were common around the early 14th, 15th and 19th century. Climate model simulations also exhibit modulation of ENSO amplitude over time. However, the extent to which this reflects a forced response remains uncertain. Key differences among reconstructions make it challenging to assess the likelihood of changes in ENSO event frequency or diversity. We suggest that ensembles of pre-instrumental records, similar to climate model projections, may provide a way forward for improving our understanding of past ENSO variability. Future work that carefully selects or develops proxy records in a way that, for example, targets ENSO diversity or teleconnection stability over time will also lead to further progress.

This article is categorized under:

Paleoclimates and Current Trends > Paleoclimate

Paleoclimates and Current Trends > Modern Climate Change

Paleoclimates and Current Trends > Climte Forcing

## 1 | Introduction

The El Niño/Southern Oscillation (ENSO) has far-reaching and near global-scale impacts on societies and ecosystems (Alizadeh 2024; Diaz and Markgraf 1992; Lin and Qian 2019; Philander 1990; Wyrtki 1975). Driven by large-scale interactions between the oceans and the atmosphere that occur primarily across the tropical-subtropical Pacific Ocean (Rasmusson and Carpenter 1982), ENSO oscillates between three main states. These include warm (El Niño), cool (La Niña) and neutral phases. ENSO significantly influences the climate in many parts of the world, with the nature and

severity of its impacts depending on other prevailing conditions (Alizadeh 2024; Kahya and Dracup 1993; Lin and Qian 2019; McBride and Nicholls 1983; Moss et al. 1994; Peel et al. 2001; Philander 1990; Piechota et al. 1997; Rajagopalan et al. 2000; Ropelewski and Halpert 1987; Tapper and Hurry 1993; Taschetto et al. 2020). El Niño conditions are typically associated with drought in the north west of the United States, eastern Australia, southern Africa, and Indonesia (Dunbar 2000; Piechota and Dracup 1996), while La Niña conditions are commonly associated with drought in the southwestern United States (Allen and Anderson 2018) and floods in parts of Asia and Australia (Lieber et al. 2024; McGregor et al. 2024; Ward, Eisner, et al. 2014). Socio-economic impacts include effects on fishing industries (Bertrand et al. 2020), global crop yields (Phillips et al. 1998; Potgieter et al. 2002; Rimmington and Nicholls 1993; Sazib et al. 2020; Yuan and Yamagata 2015), and the economic costs associated with managing natural disasters like mudslides and flooding in the southern United States, central South America, the horn of Africa and parts of Eurasia (Corringham and Cayan 2019; Ward, Jongman, et al. 2014). However, ENSO events differ in their impacts from one to the other (L'Heureux et al. 2024), and their return frequency is not constant (Philander 1990; Timmermann et al. 2018).

Due to the widespread implications of the phenomenon, scientific interest in ENSO has been high and our understanding of the system's complexity has evolved rapidly over the past 30 years (Cai et al. 2021; Guilyardi et al. 2020). We now understand that ENSO is modulated by internal variations operating across a range of timescales. At the decadal to multidecadal scale, ENSO is influenced by low-frequency modes such as the Interdecadal Pacific Oscillation (IPO; England et al. 2014; Henley 2017; Newman et al. 2016; Power et al. 1999; Schlör et al. 2024; Trenberth and Stepaniak 2001) and related modes like the Pacific Decadal Oscillation (PDO), which share overlapping spatial and temporal characteristics (Capotondi et al. 2023; Okumura et al. 2017; Power et al. 2021). These low-frequency variations present key challenges due to their interaction with ENSO and complicate efforts to disentangle natural variability from external forcing, as changes in mean state occur at multiple timescales (Chung and Li 2013; Kosaka and Xie 2013; Li et al. 2020; Liguori and Lorenzo 2018; Martín-Gómez et al. 2024; Wills et al. 2018).

At shorter timescales, ENSO is modulated by intraseasonal variability such as the Madden-Julian Oscillation (MJO; Hendon and Salby 1994; Jiang et al. 2020), which not only influences ENSO but is also modulated by it (Dasgupta et al. 2021; Shimizu and Ambrizzi 2016). ENSO also interacts with the Indian Ocean and Atlantic Ocean basins in complex and multifaceted ways. Sea surface temperatures within these basins influence regional climate and can, in turn, exert feedbacks that affect ENSO evolution (Cai et al. 2019; Ham et al. 2013; Kug and Kang 2006; Wu et al. 2005). These basin interactions are mediated by atmospheric processes such as the Walker circulation and the atmospheric bridge mechanism, which transfers ENSO signals across both the tropics and the extratropics, particularly the North Pacific (Alexander et al. 2002; Schott et al. 2009) and the South Pacific through the South Pacific Meridional mode (Chiang and Vimont 2004; Sanchez et al. 2019; Zhang et al. 2013).

External forcings, such as volcanic eruptions and solar variability, can also modulate ENSO-related feedbacks. For example, it has also been proposed that volcanic eruptions (see McGregor et al. (2020) and references within) and solar variability affect ENSO through their impacts on atmospheric and oceanic conditions that govern its dynamics, although links between these external forcings and ENSO remain a topic of active debate (Adams et al. 2003; Cai et al. 2021; Cobb et al. 2013; Dee et al. 2020; Handler 1984; Jiang et al. 2023; McGregor et al. 2020; Wilcox et al. 2023; Zhu et al. 2022). Additionally, anthropogenic climate change introduces new complexities for predicting ENSO behavior because rising global temperatures may alter the frequency, intensity, teleconnections, and characteristics of ENSO events (Alizadeh 2024; Cai et al. 2023, 2021, 2020, 2015, 2018; Fredriksen et al. 2020; Hendon et al. 2009; Lieber et al. 2024; Maher et al. 2022; Maher et al. 2023; Timmermann et al. 2018).

'ENSO diversity' adds further complexity to ENSO dynamics. ENSO events are associated with distinct patterns of sea surface temperature (SST) warming (Capotondi et al. 2015; Johnson 2013; Kug et al. 2009; Larkin and Harrison 2005; Timmermann et al. 2018; Yeh et al. 2014). These differences result in varying temperature and precipitation teleconnections globally. Eastern Pacific (EP) El Niño events occur when warming is greatest in the eastern Pacific whereas for a Central Pacific (CP) event, warming is greatest in the central tropical Pacific (Ashok et al. 2007; Kao and Yu 2009; Kug et al. 2009; Larkin and Harrison 2005; Yeh et al. 2014; Yu and Kim 2013). While it is possible to define different types of La Niña events based on the location of SST cooling, the respective teleconnections are much less varied compared to EP and CP El Niño events (Schlör et al. 2023; Wiedermann et al. 2021; Yuan and Yan 2013). Recognition of ENSO diversity has challenged our understanding of recent (Newman et al. 2011; Yeh et al. 2009), and, by extension, projected changes in ENSO behavior (Chen et al. 2016; Freund et al. 2020; Freund et al. 2024; Kim and Yu 2012; Taschetto et al. 2014). Additionally, our understanding of the asymmetry of impacts of La Niña and El Niño events Cai et al. (2010); DeLong et al. (2012); Frauen et al. (2014), and how this relates to ENSO diversity (Ren et al. 2022) and its modulation by other factors is still evolving (Sengupta et al. 2025).

The greatest limitation to understanding the complexity around ENSO is the limited number of observed events in the short instrumental record, prohibiting generalizations about ENSO properties (Diamond and Bennartz 2015; Wittenberg 2009). Notably, very strong events (such as the 1972/73, 1982/83, 1997/98, and 2015/16 El Niños and the 1973/74, 1988/89, 2007/08, and 2010/11 La Niñas (Santoso et al. 2017)) occur infrequently and are therefore under-represented in our instrumental data. These extreme events are distinguished by their unique dynamical characteristics, such as unusually strong westerly wind bursts or extensive eastward displacement of warm water masses, as well as their significant socio-economic and environmental impacts (Liu et al. 2023). Such events have been central to advancing our understanding of ENSO dynamics, highlighting the need for extended (ideally multi-century) datasets. In an attempt to address this deficiency, over the past ~30 years, a number of ENSO reconstructions (Table 1) have been developed (derived from both natural archives

**TABLE 1** | Overview of available ENSO related reconstructions.

| Study | Abbr. | Target index or region | Target season | Time span | Archives | Proxy locations | Method | Notes |
|---|---|---|---|---|---|---|---|---|
| Quinn et al. (1978) | | NA | NA | 1861–1976 | Documentary | Peru | Qualitative | El Niño in 4 categories |
| Quinn and Mayolo (1987) | | NA | NA | 1525–1982 | Documentary | Ecuador, Peru, and Pacific | Qualitative | El Niño in 4 categories |
| Quinn and Neal (1992) | | (SOI) | NA | 622–1992 | Documentary | Ecuador, Peru, and Pacific | Qualitative | El Niño in 6 categories |
| Quinn and Quinn (1993) | | NA | NA | 1525–1992 | Documentary | Ecuador, Peru, and Pacific, Nile River | Qualitative | El Niño in 6 categories and confidence rating(1–5) |
| Garcia-Herrera et al. (2008) | | NA | NA | 1550–1900 | Documentary | Northern Peru, Trujillo | Qualitative | El Niño chronology derived from precipitation impact |
| Brönnimann et al. (2007) | | NA | NA | 1500–2005 | Multi-archive | Tropical Pacific, North Atlantic-European region, and surrounding areas | Data set compilation | Combination of reconstructions, instrumental data, and compositing methods |
| Gergis and Fowler 2005 | | CEI | Annual | 1525–2002 | Multi-archive | Multiple sources | Data set compilation | El Niño and La Niña events |
| Stahle and Cleaveland (1993) | S93 | SOI | Oct–Mar | 1699–1971 | Tree-ring | USA, Mexico | Regression | |
| Stahle et al. (1998) | S98 | SOI | Dec–Feb | 1706–1977 | Multiproxy | Pacific rim | PCR | |
| Mann et al. (2000) | Man | Niño3 | Oct–Mar | 1650–1980 | Multiproxy | Near-global | Regression | |
| Cook et al. (2008) Niño12 | | Niño12 | Dec–Feb | 1300–2006 | Tree-rings | Mexico, Texas | | |
| Cook et al. (2008) Niño3 | | Niño3 | Dec–Feb | 1300–2006 | Tree-rings | Mexico, Texas | | |
| Cook et al. (2008) Niño4 | | Niño4 | Dec–Feb | 1300–2006 | Tree-rings | Mexico, Texas | | |
| Cook et al. (2008) Niño34 | Coo | Niño34 | Dec–Feb | 1300–2006 | Tree-rings | Mexico, Texas | | |
| D'Arrigo et al. (2005) Niño3 | DAr | Niño3 | Dec–Feb | 1408–1978 | Tree-rings | Subtropical North America | PCR | |
| Braganza et al. (2009) Multiproxy R5 | Bra | (SOI, CEI, Niño3.4) | Multiple (Nov–Apr) | 1727–1982 | Multiproxy | Pacific rim | PC1 | Five proxy records |

(Continues)

**TABLE 1** | (Continued)

| Study | Abbr. | Target index or region | Target season | Time span | Archives | Proxy locations | Method | Notes |
|---|---|---|---|---|---|---|---|---|
| Braganza et al. (2009) Multiproxy R8 | Bra | (SOI, CEI, Niño3.4) | Multiple (Nov–Apr) | 1525–1982 | Multiproxy | Pacific rim | PC1 | Eight proxy records |
| McGregor et al. (2010) | McG | UEP$^{+}$ (Niño3) | Jul–Jun | 1650–1977 | Multiproxy | Mid- and tropical latitudes, near global | PCR | |
| Wilson et al. (2010) Niño34 COAPCR | WC | Niño3.4 | Dec–Nov | 1541–1997 | Multiproxy | Pacific basin | PCR | |
| Wilson et al. (2010) Niño34 COACPR | | Niño3.4 | Dec–Nov | 1541–1997 | Multiproxy | Pacific basin | CPR | |
| Wilson et al. (2010) Niño34 zscoreCOA | | Niño3.4 | Dec–Nov | 1541–1997 | Multiproxy | Pacific basin | zscore | |
| Wilson et al. (2010) Niño34 TelePCR TEL | WT | Niño3.4 | Dec–Nov | 1607–1997 | Multiproxy | Pacific/Indian Ocean regions | PCR | |
| Wilson et al. (2010) Niño34 zscore TEL | | Niño3.4 | Dec–Nov | 1607–1997 | Multiproxy | Pacific, Indian basins | zscore | |
| Wilson et al. (2010) Niño34 TeleREGEM TEL | | Niño3.4 | Dec–Nov | 1997–2011 | Corals | Pacific, Indian basins | RegEM | Teleconnected proxies |
| Li et al. (2011) NADA PC1 | L11 | (Niño3) | Jan–Mar | 900–2006 | Tree rings | Tropics/midlatitudes | PCR | Uses drought atlases (NADA, MADA) based on Jun–Aug conditions |
| Emile-Geay et al. (2013a, 2013b) Niño34 | Gea | Niño3.4 | Dec–Feb | 1150–1995 | Multiproxy | Near-global | RegEM | Niño34 ERSST |
| Li et al. (2013) PC1 NADA, MADA other tree-rings | L13 | (Niño3.4) | Nov–Jan | 1301–2005 | Tree rings | Tropics/midlatitudes | PCR | Uses drought atlases (NADA, MADA) based on Jun–Aug conditions |
| Tierney et al. (2015) East | TE | Eastern Pacific SSTs | Apr–Mar | 1617–2006 | Coral | Pacific, Indian Ocean | CPS | Average SST East Pacific |
| Tierney et al. (2015) West | TW | Pacific Warm Pool | Apr–Mar | 1607–1998 | Coral | Pacific, Indian Ocean | CPS | Average SST West Pacific |
| Torbenson et al. (2019) eMEIstable | Tor | MEI | Nov–Feb | 1675–1994 | Tree rings | Southwestern USA/Mexico | PCR | |
| Torbenson et al. (2019) eMEIall | | MEI | Nov–Feb | 1675–1994 | Tree rings | Southwestern USA/Mexico | PCR | |

(Continues)

**TABLE 1** | (Continued)

| Study | Abbr. | Target index or region | Target season | Time span | Archives | Proxy locations | Method | Notes |
|---|---|---|---|---|---|---|---|---|
| Freund et al. (2019) NCT DJF | FCT | NCT | Dec–Feb | 1617–2008 | Coral | Tropical Pacific, Indian ocean | PCR | Seasonal reconstruction |
| Freund et al. (2019) NWP DJF | FCT | NWP | Dec–Feb | 617–2008 | Coral | Tropical Pacific, Indian ocean | PCR | Seasonal reconstruction |
| Freund et al. (2019) Niño3 DJF | | Niño3 | Dec–Feb | 1617–2008 | Coral | Tropical Pacific, Indian ocean | PCR | Seasonal reconstruction |
| Freund et al. (2019) Niño4 DJF | | Niño4 | Dec–Feb | 1617–2008 | Coral | Tropical Pacific, Indian ocean | PCR | Seasonal reconstruction |
| Dätwyler et al. (2019) FullPeriod PC1 | D19 | Niño3.4 | Jan–Dec | 1000–1990 | Multiproxy | Near global | PC1 | |
| Dätwyler et al. (2020) ENSO DJF | D20 | Niño3.4 | Dec–Feb | 1000–1990 | Multiproxy | Near-global | PCR | |
| Zhu et al. (2022) Ocn2kCorals Li3b6 | Zhu | Niño3.4 | Dec–Feb | 1100–2000 | Corals | Pacific, Atlantic | LMR | Paleoclimate data assimilation |
| Zhu et al. (2022) Corals Li3b6 | | Niño3.4 | Dec–Feb | 1100–2000 | Corals | Pacific, Atlantic | LMR | Paleoclimate data assimilation |
| Zhu et al. (2022) Li3b6 | | Niño3.4 | Dec–Feb | 1100–2000 | Tree-rings | Pacific-rim | LMR | Paleoclimate data assimilation |
| Liu et al. (2024) PCR | Liu | Niño3.4 | Dec–Feb | 1190–1996 | Multiproxy | Near-global | PCR | Stable oxygen isotopes |
| Liu et al. (2024) DD | | Niño3.4 | Dec–Feb | 1190–1996 | Multiproxy | Near-global | DCC | Stable oxygen isotopes |
| Falster et al. (2023) | | ΔSLP | Annual | 1200–2000 | Multiproxy | Near-global | Various | Walker cell reconstructions mostly based on stable oxygen isotopes |

*Note:* Gray indicates reconstructions examined further in this article. Target season does not necessarily reflect the season which, for example, ENSO was reconstructed (see notes). Where an index is enclosed in parentheses, the reconstruction has been scaled to, or associated with, that index although the index itself was not specifically targeted. Braganza et al. (2009) comment that their reconstruction is closely aligned with Niño3.4, the Southern Oscillation Index and a combined Ocean–atmosphere Index. The same study also examines relationships across a range of seasons including the Nov–Apr season with one of the highest associations with Niño3.4, hence the 'multiple (Nov–Apr)' entry in the Target season column. [+]indicates that this index was developed by the McGregor et al. (2010) study, not targeted. Note that the instrumental period of the Emile-Geay et al. (2013a) reconstruction is actually the instrumental data itself. Additionally, we have not listed individual documentary records compiled by Gergis and Fowler (2009) please consult that publication for details.

and documentary records) that can provide insights into ENSO characteristics during the last millennium and contextualize observations over the 20th and early 21st Centuries (e.g., (Freund et al. 2019; Liu et al. 2017; Tierney et al. 2015)). In addition, General Circulation Models (GCMs) have been employed to simulate past ENSO behavior in pre-industrial periods. These models provide a valuable tool for understanding the fundamental processes governing ENSO dynamics and how they may have varied under different background climate states.

Climate change over the last millennium is relatively small compared with changes on longer timescales; for example, early and mid-Holocene climates experienced very different seasonal insolation, while glacial climates were globally colder with altered atmospheric and oceanic circulation and temperature gradients. Exploring ENSO changes in these very different Holocene and glacial past climates provides valuable insights into ENSO sensitivity to changes in the mean state (Brown et al. 2020; Emile-Geay et al. 2015; Karamperidou et al. 2015). However, high-resolution proxy records suitable for reconstructing ENSO in these past climates are limited, while records spanning the last millennium are more plentiful. We therefore focus this review on the last millennium period, while noting that extending the ENSO record back further in time should be a goal of future proxy and modeling efforts.

In this review we collate and present an overview of interannual ENSO variability over the past millennium for a broad audience. Because palaeo-ENSO reconstructions are typically based on specific ENSO indices, we begin by providing an overview of ENSO and how it is represented through various SST and sea level pressure (SLP) measurements. We then review continuous interannual ENSO reconstructions and discrete ENSO event reconstructions as well as ENSO in GCMs. The representation of key ENSO features, including temporal evolution and spatial patterns, is systematically compared across the individual continuous reconstructions. This comparison involves analyzing the reconstructions' ability to capture ENSO's interannual variability, low-frequency modulation, and spatial teleconnection patterns, as well as different types of El Niño patterns. Similarly, common ENSO events are identified from the discrete ENSO event reconstructions by focusing on years where multiple records agree on the occurrence of El Niño or La Niña conditions. We point out periods of common ENSO activity and show the consistency in the classification of event strength and type among these discrete reconstructions. Lastly, we synthesize all available interannual palaeo-ENSO information, including both continuous and discrete reconstructions, to provide a comprehensive picture of ENSO during the pre-industrial era. We point towards common periods of enhanced or suppressed ENSO activity, changes in ENSO frequency or amplitude and discuss how we could better utilize palaeo-ENSO knowledge and new ENSO reconstructions.

## 2 | Basic Enso Dynamics

ENSO is a coupled ocean–atmosphere process that evolves over months to years, producing distinct responses in both the ocean and atmosphere of the equatorial Pacific Ocean (Diaz and Markgraf 1992). The mean state of the tropical Pacific exhibits significant east–west (zonal) and north–south (meridional) variations (Figure 1). The thermally driven meridional Hadley Circulation features rising air near the equator and sinking air at approximately 30° latitude in the subtropics of both hemispheres (Hadley 1735). Near the surface, air flows back towards the equator, creating a band of low surface pressure close to the equator flanked by high pressure areas in the subtropics (Figure 1a). This pressure gradient drives the transfer of sensible and latent heat, generating the characteristic surface wind patterns. The western equatorial Pacific, known as the Western Pacific Warm Pool, experiences the warmest SSTs globally. This warm pool is a significant source of moisture and heat for the atmosphere over the Maritime Continent and surrounding areas (Bjerknes 1969; Dayem et al. 2007; Kim et al. 2020; McPhaden, Santoso, and Cai 2020). Persistent easterly trade winds in the equatorial Pacific are comprised of converging northeasterly and southeasterly winds in the Northern and Southern Hemispheres respectively (Figure 1b). These convergence regions experience strong upward motion and increased atmospheric moisture convergence. The resulting zone of intense convection, known as the Intertropical Convergence Zone (ITCZ), manifests as a quasi-stationary cloud band and heavy precipitation (Figure 1b) just north of the equator (Oliver 2005). The ITCZ is flanked by arid regions to its north and the Pacific Dry Zone (PDZ) to the south (Quinn and Burt 1970). The South Pacific Convergence Zone (SPCZ), another area of substantial rainfall and moisture convergence, extends southeastward from the western Pacific warm pool. It is positioned west of the eastern Pacific subtropical high (Figure 1b) and connects with the ITCZ in its northwestern extent (Vincent 1994). The ITCZ and SPCZ are associated with the large-scale precipitation distribution across the tropical Pacific, which closely corresponds to the SST pattern in the region (Figure 1a).

During the Neutral ENSO phase, a pronounced east–west (zonal) gradient exists in both SST and atmospheric pressure across the Pacific, with warm waters and low pressure in the west, and cooler waters and higher pressure in the east. This gradient drives the Walker Circulation, a zonal atmospheric overturning circulation (Bjerknes 1969), which is coupled to both oceanic and atmospheric conditions. The ocean–atmosphere coupling forms a positive feedback loop known as the Bjerknes feedback. The east–west pressure gradient drives easterly trade winds along the equator. These winds cause westward surface currents and equatorial divergence, enhancing upwelling of cool subsurface awater in the east. Enhanced upwelling amplifies the east–west temperature gradient. The increased temperature gradient strengthens the pressure gradient, intensifying the easterly winds and the Walker Circulation, reinforcing the easterly trade winds, and completing the feedback loop. The persistent easterly winds increase stress on the ocean surface. Through Ekman transport, this stress causes further divergence of surface waters at the equator, enhancing upwelling (Penland et al. 2013). Consequently, the thermocline shoals in the east and deepens in the west, amplifying the zonal SST contrast. This self-reinforcing Bjerknes feedback can amplify initial perturbations in the tropical Pacific, modulating SSTs and atmospheric circulation. Depending on the initial perturbation, this feedback can potentially lead to the development of El Niño or La Niña events (Marshall and Plumb 2016; Trenberth 2020).

Marked variability in the tropical Pacific is associated with phases of anomalous warmer (El Niño) and colder (La Niña)

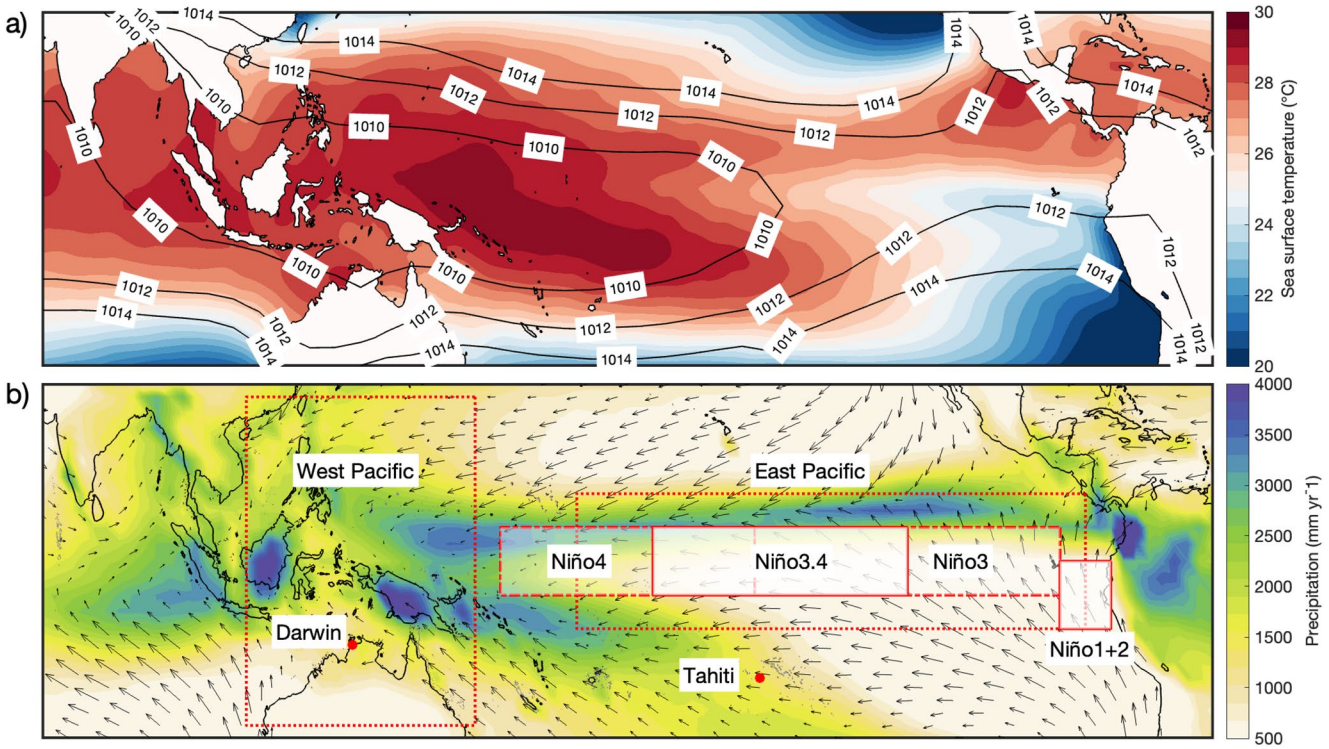


**FIGURE 1** | Tropical mean state Climatology of the tropical mean state in the Pacific for (a) sea surface temperatures (shading) and sea level pressure (isobars), (b) precipitation (shading) and wind (arrows) with highlighted different regions and the SOI index locations Darwin and Tahiti. The western Pacific (25° S–25° N and 110° E–155° E) and eastern Pacific (10° S–10° N and 175° E–85° W) regions are shown which are reconstructed by Tierney et al. (2015) along with the Niño4 region (5° S–5° N and 160° E–150° W), Niño3.4 region (5° S–5° N and 170° E–120° W), Niño3 region (5° S–5° N and 150° E–90° W) and Niño1 + 2 region (5° S–5° N and 90° W–80° W), which are often targeted by ENSO reconstructions.

SSTs (Rasmusson and Carpenter 1982). A typical ENSO event usually initiates in April/May, with the complete life cycle lasting between 12 and 24 months (Allan 1988, 2000; Ropelewski and Halpert 1987; Wright 1985). However, each ENSO event differs in terms of timing, extent, and magnitude (Wolter and Timlin 1998). During a La Niña event, a strengthening Walker circulation results in a shallower thermocline in the east but a deepening thermocline in the west due to the pressure differential across the Pacific (Figure 2b). This also leads to an amplification in the strength of the easterly trade winds and causes a greater degree of cool water upwelling along the South American west coast. This upwelling results in cooler than average SSTs in the eastern and central Pacific, and the centre of precipitation moves westwards (Sun and Bryan 2013).

Opposing processes occur during the El Niño phase when the tropical Pacific becomes anomalously warm (Figure 2c). In a canonical El Niño state, pressure over the eastern Pacific decreases while pressure in the western tropical Pacific rises (Allan et al. 1996). This pressure shift results in a weakening of the easterly trade winds and reduced upwelling off the South American coast (Figure 2a). As a result, the thermocline deepens to the east and SSTs increase and extend further east, meeting with an anomalously we ak cold tongue. The pronounced convection centre associated with the ascending branch of the Walker Circulation shifts eastward, and in extreme cases, the Walker Circulation can even reverse (Glantz 1996). The distinction between 'eastern' or 'central' Pacific El Niño events is based on the main location of warming (Figure 2c,d). While canonical EP events are characterized by strong anomalous warming in the eastern Pacific, in CP El Niño events anomalous warming occurs closer to the Central Pacific and is flanked by colder SSTAs to the east and west (Larkin and Harrison 2005). These zonal SST patterns result in an anomalous two-cell Walker Circulation that increases convection in the central Pacific (Ashok et al. 2007; Ashok and Yamagata 2009).

## 3 | Measuring Enso

Several different numerical indices have been developed to capture ENSO status. The Troup Southern Oscillation Index (SOI Troup 1965) was the earliest of these indicators, and is based on the disparity in atmospheric pressure at sea-level between Tahiti and Darwin (Allan et al. 1991). The Southern Oscillation Index (SOI) is an indicator of the strength of the Walker circulation, with negative values potentially associated with El Niño conditions and positive values with La Niña conditions. Over time, a recognition that ENSO is a coupled ocean–atmosphere phenomenon emerged (Bjerknes 1969; Rasmusson and Carpenter 1982; Wyrtki 1985), with oceanic processes playing a crucial role alongside atmospheric factors, leading to the development of SST based ENSO indices. SST data were initially collated from ship log books for specific regions: Niño1, Niño2 (later combined as Niño1 + 2), Niño3, and Niño4 Figure 1. Niño3.4, located across the western and eastern parts of the Niño3 and Niño4 regions respectively, subsequently emerged as the region that best provided a representative picture of ENSO dynamics (Barnston

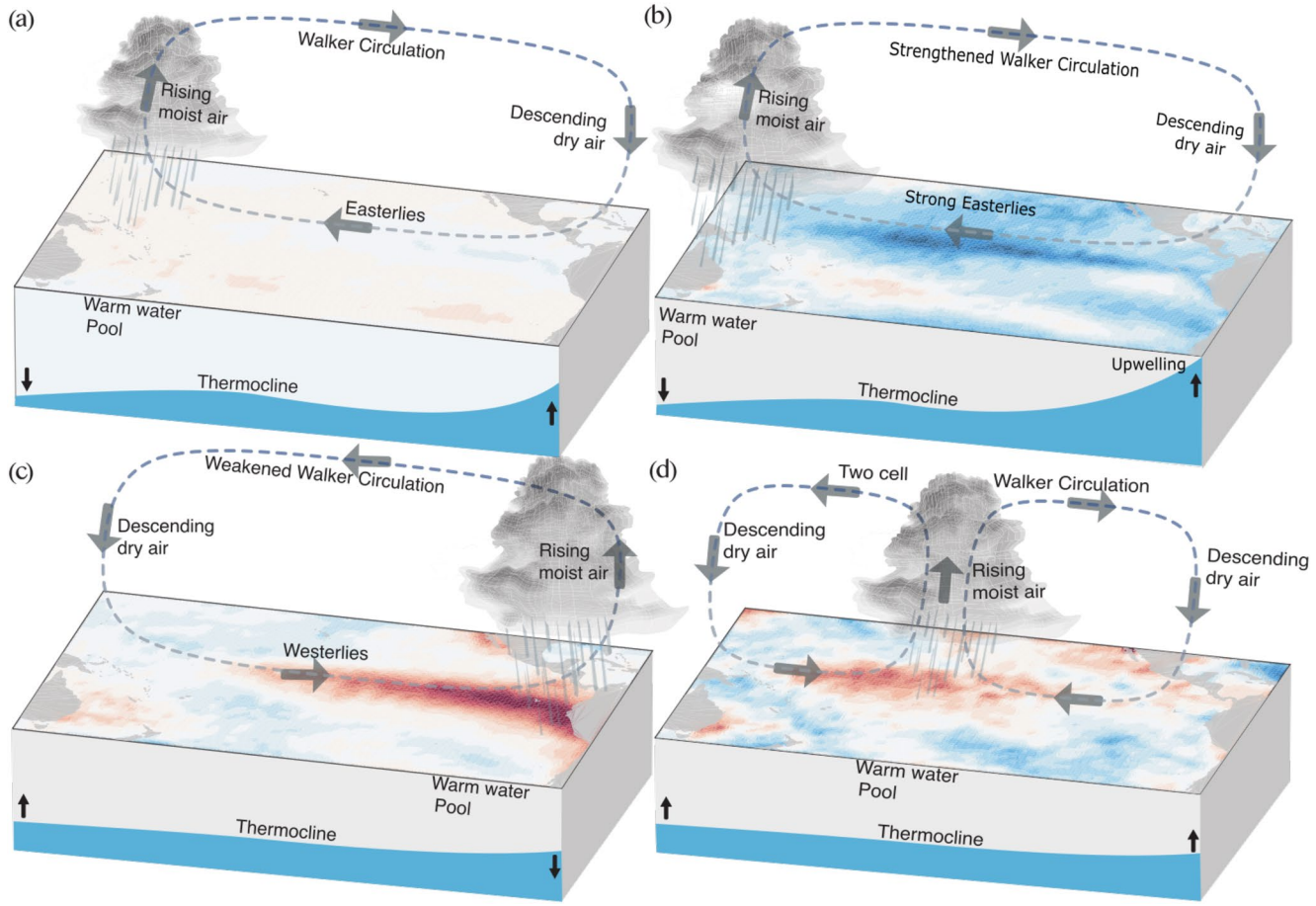


**FIGURE 2** | ENSO conditions in the tropical Pacific Schematic of neutral (a) and La Niña conditions (b), canonical eastern Pacific El Niño (c) and central Pacific El Niño (d) conditions illustrated by an idealized cross-section. Arrows indicate the change of the thermocline during ENSO events.

et al. 1997). The SSTs across these ENSO regions are expressed as anomalies (departure from the mean SST for that region and time of year). Warm SST anomalies $>0.5°C$ are generally interpreted as reflecting El Niño events, whereas cool SST anomalies of $<-0.5°C$ are interpreted as La Niña events.

ENSO monitoring also led to the development of indices that incorporate multiple oceanic and atmospheric parameters. The Coupled ENSO Index (CEI), for instance, combines information from both oceanic and atmospheric variables (Gergis and Fowler 2005). It is calculated as the difference between two regional averages between Niño 3.4 SST and the SOI index to provide a single unified index that represents the full ENSO cycle, including both the El Niño (positive CEI values) and La Niña (negative CEI values) phases. Another such index is the Multivariate ENSO Index (MEI; (Wolter and Timlin 1998)), which was originally based on six variables but has since been refined to include five: sea level pressure (SLP), SST, the zonal and meridional components of surface wind, and outgoing longwave radiation (OLR) across the tropical Pacific basin (30° S–30° N and 100° E–70° W). These multi-parameter indices aim to provide a more holistic picture of ENSO variability than indices focused solely on the atmospheric or oceanic ENSO components but require a greater amount of mainly satellite-derived input data. A comparison of the Niño indices and the MEI and SOI shows that the indices very closely reflect one another, although there are some important differences, particularly between the mixed, ocean-based and atmospheric indices (details in McPhaden, Lee, et al. (2020)). Yet other indices include a temporal criterion for designating an event as El Niño or La Niña. For example, the Oceanic Niño Index (ONI) is based a 3 month running mean of the Niño 3.4 region(5° N–5° S, 170° W–120° W) SST anomalies. El Niño or La Niña, are judged to occur only when the anomaly exceeds $\pm 0.5°C$ for at least 5 months in a row, with stronger events defined using a higher threshold of $\pm 0.8°C$.

Identifying past ENSO events relies on the availability and quality of observations in the Pacific. Historical records of the SOI have been maintained and reconstructed using data from meteorological stations in Tahiti and Darwin dating back to 1876; however, it is recognized that the Tahiti readings are likely to be less accurate prior to 1935 (Ropelewski and Jones 1987). Unlike the SOI, SST-based ENSO indices are often derived from interpolated (gridded) products. For example, the HadISST dataset (Rayner et al. 2003) comprises monthly globally complete fields of SST and sea ice concentration on a 5-degree latitude-longitude grid from 1870 to present. Nevertheless, before 1920, less than 50% of grid boxes in the Niño34 region were sufficiently observed (Freund et al. 2019). Different underlying data and methodologies mean that historical SST datasets derived from data in data-sparse regions can vary considerably, especially back in time when fewer observations were available (Sippel et al. 2024; Yasunaka and Hanawa 2010). Observational uncertainties (Diamond and

Bennartz 2015; Marathe et al. 2015) and sufficient record length (Wittenberg 2009) are especially important to consider in regard to ENSO diversity.

## 4 | Existing Pre-Industrial Enso-Related Information

There is a wide range of palaeo-information about ENSO and/or its teleconnected impacts. Here we focus on summarizing three sources of pre-industrial interannual ENSO information: (i) discrete or historical sources, (ii) continuous reconstructions of ENSO indices or related measurements derived from natural archives, and (iii) the simulation of past climate via palaeo-modeling. Discrete records are primarily related to observed impacts associated with specific El Niño or La Niña events, and are essentially lists of years in which notable events have occurred. Continuous information is based on quantitative reconstructions in which there is a value for every year in the record, including years for which conditions were neutral. Many of the continuous reconstructions are not independent of one another (e.g., Dätwyler et al. 2020; Dätwyler et al. 2019; Emile-Geay et al. 2013b; Li et al. 2013) because they include many of the same proxy records. The same is true for some of the discrete records (e.g., Gergis and Fowler 2009; Quinn 1992). Advances in climate modeling have also allowed for the simulation of ENSO during the last Millennium (850–1850 CE) through the Paleoclimate Modeling Intercomparison Project (PMIP). These climate models simulate past climate and ENSO variability. However, the simulated ENSO phase produced by a given model for a given year is not constrained to match the real-world ENSO state for that year. Instead, these simulations offer opportunities to investigate overall variability and its relationships with different forcing factors across long time periods.

### 4.1 | ENSO Records Derived From Documentary Sources (Discrete Reconstructions)

Records of past ENSO events have been derived from a variety of documentary sources (Barrett et al. 2018; Gergis et al. 2006; Quinn and Quinn 1993; Quinn and Neal 1992; Quinn et al. 1978). These records are typically derived from discrete impacts/events known to be driven by ENSO, including records of droughts (Quinn et al. 1978) and floods (Whetton and Rutherfurd 1994), mass mortality events of marine sea life, or the destruction of infrastructure due to extreme hydrological events (Quinn and Mayolo 1987). Others have been derived from ship log books describing sea conditions Barrett et al. (2018). Some studies infer the occurrence of El Niño events only (Garcia-Herrera et al. 2008; Ortlieb 2000; Quinn and Mayolo 1987; Quinn and Neal 1992), while others also include La Niña events (Gergis and Fowler 2005; Whetton and Rutherfurd 1994). Discrete records can extend back several hundred years or even further (Table 1).

One of the first ENSO records was Quinn's 1978 record (Quinn et al. 1978) which relied on historical hydrological data from across the Pacific. Early ship logs and missionary records from coastal Peru and Ecuador describing rainfall, sea conditions, and other recorded environmental conditions were used to infer El Niño occurrences. Later, the Quinn record was tentatively extended (levels of confidence provided) back to 622 AD (Quinn and Quinn 1993) using Nile River flood records. However, in many instances, these earlier events appeared to be recorded at remote locations in the Northern Hemisphere. Ortlieb (2000) revised Quinn's chronology, primarily by reinterpreting the South American sources used by Quinn and reassessing the reliability of the reports, the intensity of the events, and the data quality and its significance. The Gergis and Fowler (2009) study further advanced this work by identifying both El Niño and La Niña events by combining information from documentary records with that derived from a range of natural archives to provide a comprehensive list of ENSO events back to 1525 CE.

### 4.2 | ENSO Reconstructions Derived From Natural Archives

Here we synthesize high-resolution and continuous ENSO reconstructions that rely on multiple records. Individual records can provide valuable information about past ENSO variability (e.g., (Cobb et al. 2003); see (Emile-Geay et al. 2020) for a full list of individual records), but they may be influenced by local site-specific conditions and biases. Reconstructions using multiple records can enhance the common ENSO signal by reducing noise (Mann 2002) and can offer a robust record of ENSO behavior over time (Schroeter et al. 2020).

Coral records sensitive to SSTs from the Pacific itself are likely the most direct ENSO record (Evans and Fairbanks 1999; Evans et al. 1998, 2000). However, clear evidence of ENSO teleconnections beyond the Pacific is expressed in proxies from other regions. The hydroclimate sensitivity of tree-rings in ENSO-sensitive regions has been exploited in reconstructions of ENSO variability (D'Arrigo et al. 2005; Li et al. 2013; Stahle and Cleaveland 1993; Stahle et al. 1998). A number of reconstructions also rely on teleconnections at the near-global level (e.g., Dätwyler et al. 2020; Emile-Geay et al. 2013a; Mann et al. 2000; Wilson et al. 2010). Additionally, some reconstructions have specifically aimed to differentiate between EP and CP events (e.g., Freund et al. 2019), or target SSTs in the eastern and western Pacific that may better reflect either EP or CP events (e.g., Tierney et al. 2015). Table 1 lists the available reconstructions, highlighting the different targets and proxies used.

Continuous reconstructions have been derived solely from tree ring chronologies (e.g., D'Arrigo et al. 2005; Stahle et al. 1998; Torbenson et al. 2019) and corals (e.g., Freund et al. 2019; Tierney et al. 2015), or from a mixture of proxies including tree rings, corals, ice cores and sediments (e.g., Dätwyler et al. 2019; Emile-Geay et al. 2013a). Some reconstructions extend back only to the 18th century (Stahle and Cleaveland 1993), with others stretching back as far as 900 CE (Li et al. 2013). Continuous reconstructions are typically calibrated against a specific ENSO index. For example, Stahle et al. (1998) target the SOI while D'Arrigo et al. (2005), Emile-Geay et al. (2013a), Li et al. (2013), Wilson et al. (2010) target Niño 3.4, D'Arrigo et al. (2000), Mann et al. (2000) target Niño3 and Torbenson et al. (2019) reconstruct the MEI. Some reconstructions, however, rely on the dominant mode of variability across a set of records from regions impacted by ENSO rather than targeting a specific index (Braganza

et al. 2009; McGregor et al. 2010). This leading mode of variability is then tested for association with a specific ENSO index or indices.

The most commonly used approach to reconstructing ENSO is multivariate regression (e.g., (Mann et al. 2000)) and regression analysis on dominant modes of variability extracted from predictor pools (see Table 1). The principal component regression (PCR) reconstruction method helps to minimize noise from differences in seasonal climate responses and regional ENSO teleconnection signatures among proxies. ENSO frequently emerges as the dominant mode of variability, typically associated with the first principal component (PC1) of a multiproxy network (e.g., Braganza et al. 2009). Consequently, the time series of PC1 in these studies can serve as a proxy for past ENSO variability. The Composite Plus Scaling (CPS) method (e.g., Bradley and Jonest 1993) standardizes individual proxy records, averages them, and scales the result to match an observed target time series. The methodological simplicity of CPS and fewer statistical assumptions (such as not requiring orthogonality or normality) are key advantages of this methodology (e.g., Tierney et al. 2015). The Dynamic Calibrated Composite technique (DCC) (Kaufman et al. 2020) applied by Liu et al. (2024) provides more flexible and robust integration of diverse datasets. RegEM (Regularized Expectation Maximization) is another reconstruction method that imputes missing proxy data back in time (Schneider 2001). The method works by iteratively estimating the mean and covariance structure of the complete dataset, including both observed and missing values and has been used to reconstruct ENSO indices back in time (e.g., (Emile-Geay et al. 2013a; Wilson et al. 2010)). Each reconstruction method offers distinct advantages depending on the characteristics of the underlying proxy dataset. Some techniques may be more effective at filtering non-relevant signals, while others are known to better preserve signal magnitudes. Inevitably, reconstructions differ due to variations in proxy datasets or methodological approaches. To mitigate these differences and assess methodological impacts, it is advisable to employ multiple reconstruction techniques, as demonstrated by studies such as (Emile-Geay et al. 2013a) and (Braganza et al. 2009) or for the Walker circulation (Falster et al. 2023). A multi-method approach can provide a more comprehensive understanding of past climate variability and the uncertainties associated with different reconstruction techniques.

### 4.3 | Palaeo Modeling of the Last Millennium

Climate models have been used to explore past ENSO variability for a wide range of periods including the last millennium. The skill of coupled climate models in simulating some aspects of ENSO has improved in recent generations of models (Cai et al. 2021; Hou and Tang 2022), allowing models to be used to explore ENSO sensitivity to changes in external forcing and tropical Pacific mean state. Simulations of the climate of the last millennium have been carried out as part of the Paleoclimate Modeling Intercomparison Project phases 3 (PMIP3) (Braconnot et al. 2012) and 4 (PMIP4) (Jungclaus et al. 2017). These simulations are forced with time-varying boundary conditions, including orbital parameters, greenhouse gases, volcanic forcing and solar irradiance (Jungclaus et al. 2017), providing a simulation of the evolution of climate from 850 to 1850 CE including ENSO variability. Evaluation of ENSO in PMIP3 simulations of the last millennium found decadal to centennial modulation of ENSO behavior (Lewis and LeGrande 2015). Comparison of ENSO strength and zonal mean SST gradient in PMIP3 last millennium simulations displayed a diversity in the strength and direction of the relationship (Wyman et al. 2020). Models also simulate changes in ENSO characteristics in response to strong volcanic eruptions between 1250 and 1600 CE (Lewis and LeGrande 2015). Another study of ENSO in the PMIP3 last millennium simulations found no common change in ENSO variance across models, but regional ENSO teleconnections in each model varied with ENSO strength (Brown et al. 2016). Some models also simulate an increased variability of Niño3.4 SSTs at decadal (8–25 year) frequencies following major volcanic eruptions such as at 1258 and 1452 (Hope et al. 2017).

Simulations of the last millennium have been produced as part of several large ensemble projects, including the Community Earth System Model Last Millennium Ensemble (CESM LME) (Otto-Bliesner et al. 2016). The CESM LME includes simulations with individual forcings, allowing evaluation of the influence of external forcing versus internal variability in past climate changes. In these simulations, there are no significant forced changes in ENSO amplitude but changes in ENSO diversity are detected (Stevenson, Capotondi, et al. 2019), with orbital changes having an influence on the proportion of CP versus EP El Niño events. A study of Indo-Pacific coupling over the last millennium also used CESM LME simulations (Abram et al. 2020), finding that periods of low Indian Ocean Dipole variability were associated with low Niño3.4 SST variability and a La Niña-like mean state, whereas periods of high Indian Ocean Dipole variability were associated with higher Niño3.4 SST variability and El Niño-like mean SST anomalies. CESM LME simulations have been used to investigate the response of ENSO to volcanic eruptions, with the large number of realizations of last millennium climate allowing the range of ENSO post-eruption responses to be compared (Stevenson et al. 2016). This comparison revealed the complex interaction between hydroclimate responses to volcanic eruptions and ENSO teleconnections, as well as the distinct responses of Northern and Southern hemispheres to eruptions (Stevenson et al. 2016). The occurrence of mega-droughts and mega-pluvials during the last millennium was also found to be modulated by ENSO and volcanic activity as well as Atlantic multidecadal variability based on the CESM LME simulations (Stevenson et al. 2018).

Climate models with water isotope tracers have also been used to simulate the climate of the last millennium (Brady et al. 2019; Buhler et al. 2022; Stevenson, Otto-Bliesner, et al. 2019). An isotopically-enabled version of CESM was used to carry out several single and multiple forcing last millennium simulations, producing the first isotopic Last Millennium Ensemble (Brady et al. 2019; Stevenson, Otto-Bliesner, et al. 2019) which was used to examine isotopic responses to volcanic eruptions and ENSO variability. A set of five coupled models with water isotope tracers also produced simulations of the last millennium that were compared with available speleothem records (Buhler et al. 2022).

## 5 | Characteristics of Enso Reconstructions From Natural Archives and Documentary Records

### 5.1 | Co-Variability Among ENSO Reconstructions

In some cases, multiple ENSO reconstructions have been produced within the same study by using multiple reconstruction methods (e.g., Wilson et al. 2010), targeting different indices (e.g., Cook et al. (see Table 1)) or different proxies (e.g., Braganza et al. 2009). To provide an overview of commonalities among the reconstructions, we present a dendrogram based on the covariance among the reconstructions (Figure 3). Clustering was performed using hierarchical agglomerative clustering with the average linkage method (Murtagh and Legendre 2014). ENSO reconstructions that merge at lower vertical distances are more similar in terms of their covariance structure, while those that merge at higher levels are more dissimilar. The Falster et al. (2023) Pacific Walker circulation reconstruction stands out as highly distinct from all ENSO reconstructions in the dendrogram. It forms its own branch at a much higher linkage distance, indicating low covariance similarity. This distinct clustering suggests that the Walker circulation represents a related but different aspect of tropical climate variability compared to ENSO reconstructions. The most prominent division among the ENSO reconstructions in the dendrogram separates two major clusters: the right main branch (1) contains the coral-based East Pacific SST reconstruction (Tierney et al. 2015) and the "Centre of Action" (COA) reconstructions from (Wilson et al. 2010) (orange), while the other main branch (2) contains all remaining ENSO reconstructions. This split occurs at the highest level of the dendrogram and likely reflects differences in proxy type and spatial focus. Both the COA and East Pacific reconstructions rely heavily on coral records from the eastern tropical Pacific, which may explain their close association and distinct separation from the other reconstructions. Within the larger cluster of remaining ENSO reconstructions, further sub-clustering reflects shared proxy networks or methodological similarities. For example, the Tierney West reconstruction (Tierney et al. 2015) clusters with the Zhu et al. (Zhu et al. 2022) coral network and Freund et al. (Freund et al. 2019) in a subcluster (2.1), likely due to their common use of proxies near the dateline. Another subcluster (2.2) groups the teleconnected reconstructions from (Wilson et al. 2010) and Datwyler et al. (Dätwyler et al. 2019), suggesting consistency in the use of remote proxies. The Cook reconstructions (highlighted in green) form a tight cluster at the lower end of the dendrogram, indicating high covariance among them. This suggests that targeting different ENSO indices had little impact on the overall structure of these tree-ring-based reconstructions. Likewise, the (Wilson et al. 2010) reconstructions (orange), which use different statistical methods (e.g., PCR, z-score, REGEM), also cluster closely, implying that reconstruction method had minimal influence on their shared variability. Overall, the dendrogram highlights that proxy type and spatial targeting, particularly the use of coral-based COA proxies versus teleconnected tree-ring records, are key drivers of similarity among the ENSO reconstructions.

We use this dendrogram to select representative continuous reconstructions on which we will focus for the remainder of this article. If an individual study produced multiple reconstructions, we selected one or at most two distinct reconstructions from that study. By doing this, we aim to reduce apparent

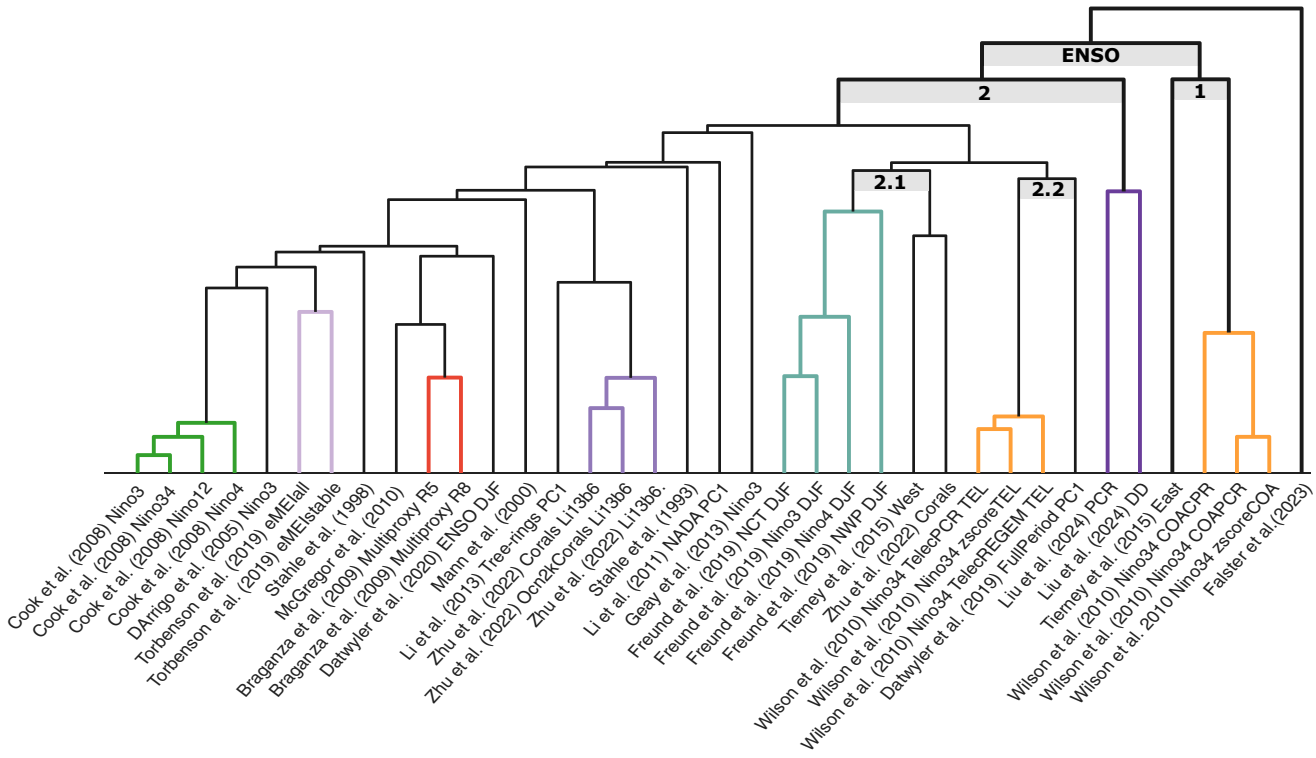


**FIGURE 3** | Dendrogram of the different ENSO reconstructions. Dendrogram of 38 ENSO reconstructions (see Table 1 for details) clustered by the covariance of records during the common pre-instrumental period (1727–1900). Reconstructions from the same study are indicated by matching line colors. The Walker Cell reconstruction by Falster et al. (2023) forms its a separate branch from all ENSO reconstructions which have two major clusters (1 and 2) and some subclusters mentioned in the text are highlighted in gray.

redundancy (as encapsulated in high covariance among reconstructions from the same study) and to better emphasize the larger differences among the reconstructions. The 20 selected reconstructions are identified by shading in Table 1 and plotted in Figure 4. From herein, where comparison is made between the 20 reconstructions and instrumental data, we focus on the Austral summer/Boreal winter (i.e., DJF) season. This choice reflects the fact that all but one reconstruction (D19) either targets or is associated with a seasonal window that includes DJF. Using a common season simplifies comparison and aligns with the timing of peak ENSO activity. While some reconstructions span broader seasonal windows, we reason that they still capture variance during DJF, making this a reasonable basis for comparison. However, when using individual reconstructions in isolation, particularly for regional impact studies or model evaluation, it may be more appropriate to refer to the specific seasonal window targeted by that reconstruction, as listed in Table 1. This ensures that comparisons are seasonally consistent with the original reconstruction methodology and proxy sensitivity.

### 5.2 | Correlation Between Paired Reconstructions

Although intercorrelations should not be considered an indicator of robustness of individual ENSO reconstruction, they highlight

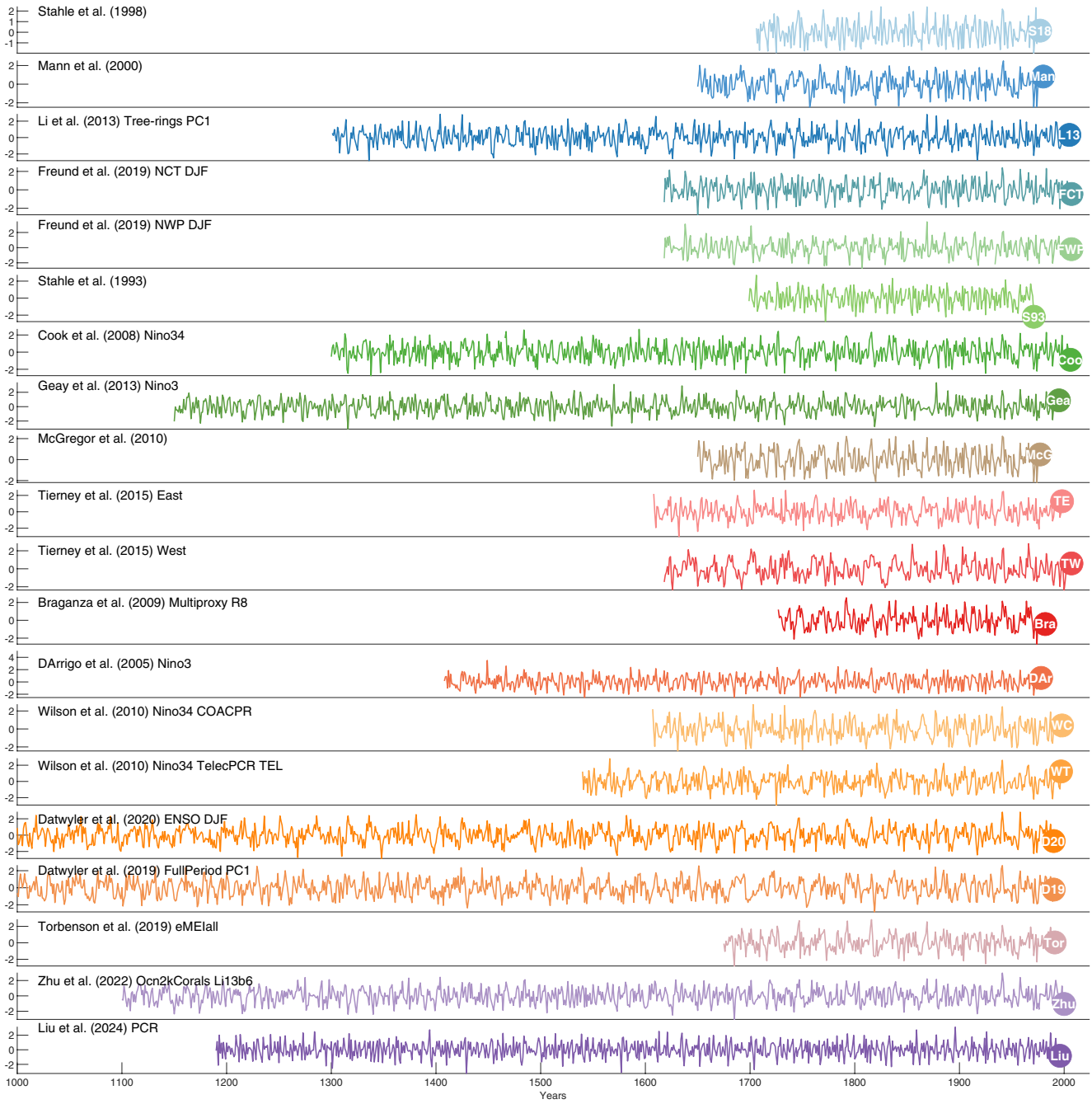


**FIGURE 4** | Time series of selected ENSO reconstructions. Time series plots of ENSO reconstructions as z-score relative to the instrumental period (1900–1971). Abbreviations shown in filled circles are used within the text.

some important commonalities and differences. The clearest result shown for the selected continuous ENSO reconstructions is that correlations between paired series are higher in the instrumental (1900–1971) than the pre-instrumental (1727–1899) period (Figure 5). These stronger instrumental-period correlations reflect the strong correlations among the target indices. Generally weaker inter-series relationships over the pre-instrumental period likely reflect differences in the mix of underlying proxy records used and changes in proxy pools over time, as well as non-climatic noise within individual records, loss of high-quality proxies, and uncertainties introduced by calibration and methodological choices during reconstruction. For example, the correlation between TW and TE is $r = 0.5$ during the instrumental period and $r = 0.01$ in the pre-instrumental periods. The much weaker correlation back in time may reflect changes in the proxy-climate relationship or the inherent limitation of a shrinking proxy pool back in time, something that affects most multi-proxy reconstructions. The relatively stable relationships between the multi-proxy *Bra* (Braganza et al. 2009) that relies on the same eight proxies for its entire length and the remaining reconstructions over both the instrumental and pre-instrumental periods offers some support to the idea that diverging signals are partly related to a shrinking proxy pool (and hence decreasing signal) back in time. A number of other reconstructions still exhibit moderately strong relationships with many others across both periods (e.g., Zhu, Tor, D20, Figure 5).

One reason why stronger correlations between several large-scale multi-proxy reconstructions (e.g., McG, Gea, D20) and the remaining reconstructions may exist is that they include many of the proxies used by the reconstructions relying on a smaller proxy record pool. In contrast, D19, S93, WT, WC, and TW have some of the weakest correlations with other reconstructions. Notably, S93 targets the SOI, D19 and WT/WC use unusual seasonal windows (January–December and December–November), while TW is for the Pacific Warm Pool rather than the Niño3.4 or 3 regions. Liu also shows generally weak relationships with most other reconstructions during the pre-instrumental period (Figure 5). These weak correlations may partly reflect preprocessing choices applied to proxy records, such as the use of filters (e.g., a 9-year high-pass Butterworth filter (Liu et al. 2024)), which can affect variability and inter-series relationships. In addition, the relatively coarse temporal resolution of the oxygen isotope proxy records (approximately 2 years; e.g., tree rings and speleothems) used in the Liu reconstruction may further contribute to reduced correlation.

Weaker inter-series relationships over the pre-instrumental period can stem from various factors, including dating uncertainties such as missing, false, or double counted years (DeLong et al. 2013) within the proxy pool used to reconstruct ENSO. Even small dating errors of 1–2 years can disrupt interannual climate signals, weakening patterns that otherwise align well during the instrumental period due to destructive interference (Comboul et al. 2014; Emile-Geay et al. 2013a). Whilst individual proxy records bear the risk of such uncertainties, combining multiple records and proxies can mitigate this risk through cross-validation

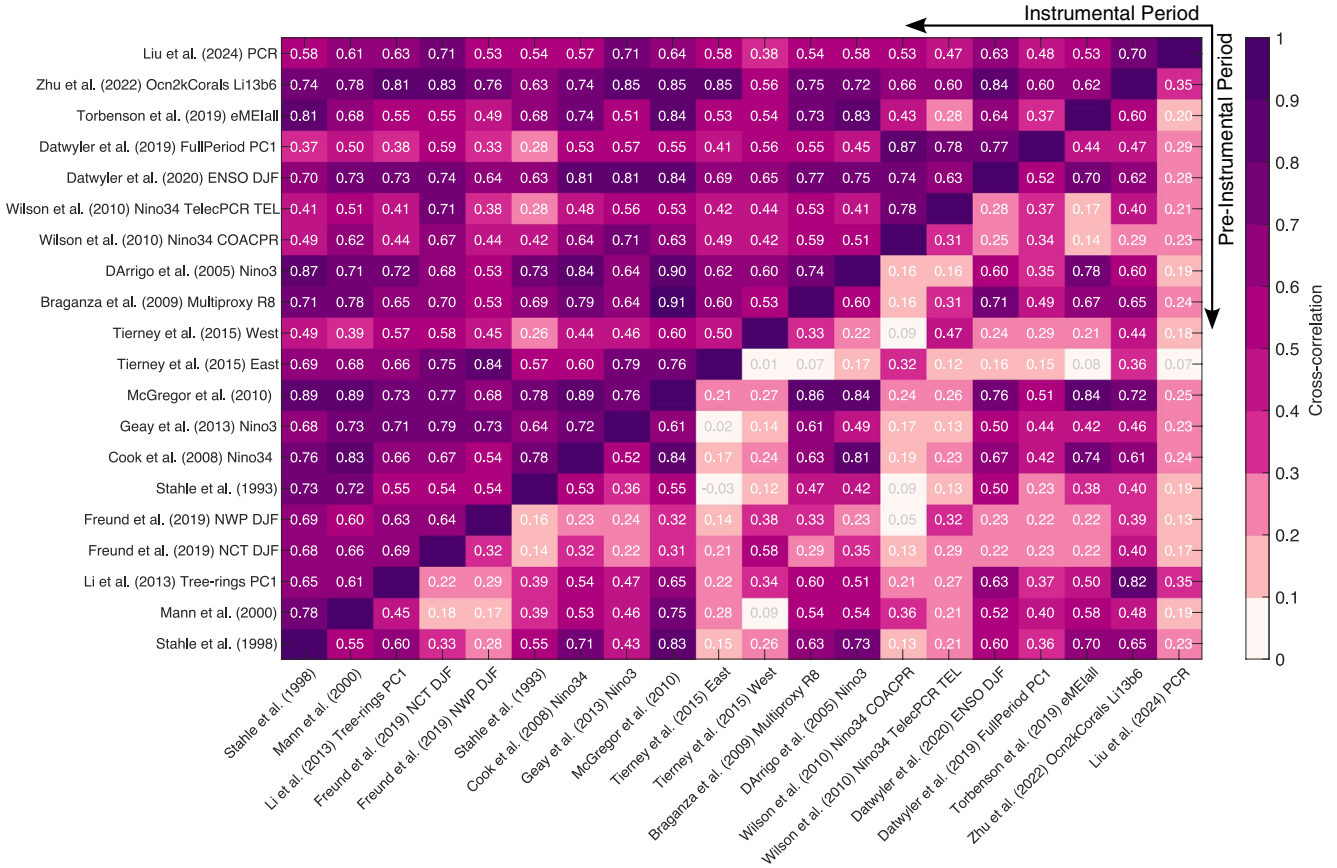


**FIGURE 5** | Heatmap of cross-correlation of ENSO reconstructions during instrumental and pre-instrumental period. Intercomparison of 20 ENSO reconstructions using cross-correlations during the common instrumental period (1900–1971) above the diagonal and the common pre-instrumental period (1727–1900) below the diagonal.

and minimizing the influence of errors inherent to any single record (Evans et al. 1998, 2002; Stevenson et al. 2013). However, as the temporal and spatial coverage of proxy records decreases further back in time, dating uncertainties become more pronounced, potentially compromising the accuracy of high-frequency and decadal climate signal reconstructions (Comboul et al. 2014). This is particularly challenging for pre-instrumental periods where cross-referencing with known data is not feasible. Consequently, the apparent divergence between reconstructions in earlier periods could be related to limitations of a shrinking proxy pool and increased dating uncertainties.

### 5.3 | Spatial Signatures

The spatial SST signatures of the reconstructions during the instrumental period are generally very similar (Figure 6). The largest differences relate to the strength of correlations with the Indian Ocean, with D19 and WT exhibiting virtually no relationship in this region. The very strong correlations between Gea and tropical Pacific SSTs are not surprising as the modern end of this reconstruction has been appended with instrumental data itself.

Compared to the relationships with SSTs, there are greater differences in the relationship between the reconstructions and the global PDSI (Figure 6). In general, significant correlations with the southwestern United States, Mexico, eastern Australia, the maritime continent, and the Indian subcontinent are observed. However, the two reconstructions specifically representing the western Pacific, TW and, to a lesser extent, FWP, are also significantly associated with drought across Eurasia. Additionally, McG and Tor are also strongly related to western Pacific SSTs and drought in parts of east Africa. This relationship is also somewhat reflected in a number of the other reconstructions (e.g., Coo and Bra).

### 5.4 | Persistence, Low Frequency Variability and Association With Instrumental Data

Perhaps one of the most difficult aspects of ENSO to quantify based solely on instrumental data is its low frequency variability. Recent work has associated multidecadal variability with ENSO diversity and the occurrence of extreme events (Fedorov et al. 2020; Schlör et al. 2024; Yeo et al. 2017). The much longer palaeo-ENSO reconstructions can provide much richer low-frequency variability information. Figure 7a shows the Hurst exponent and autocorrelation for each reconstruction and two of the key instrumental ENSO indices (SOI and Niño3.4). The Hurst exponent is a measure of long-term memory in a time series, while autocorrelation is simply a measure of the association between a time series and a delayed version of itself.

The instrumental SOI and Niño3.4 time series exhibit Hurst exponents of $H = 0.57$ and $H = 0.63$, respectively, indicating some

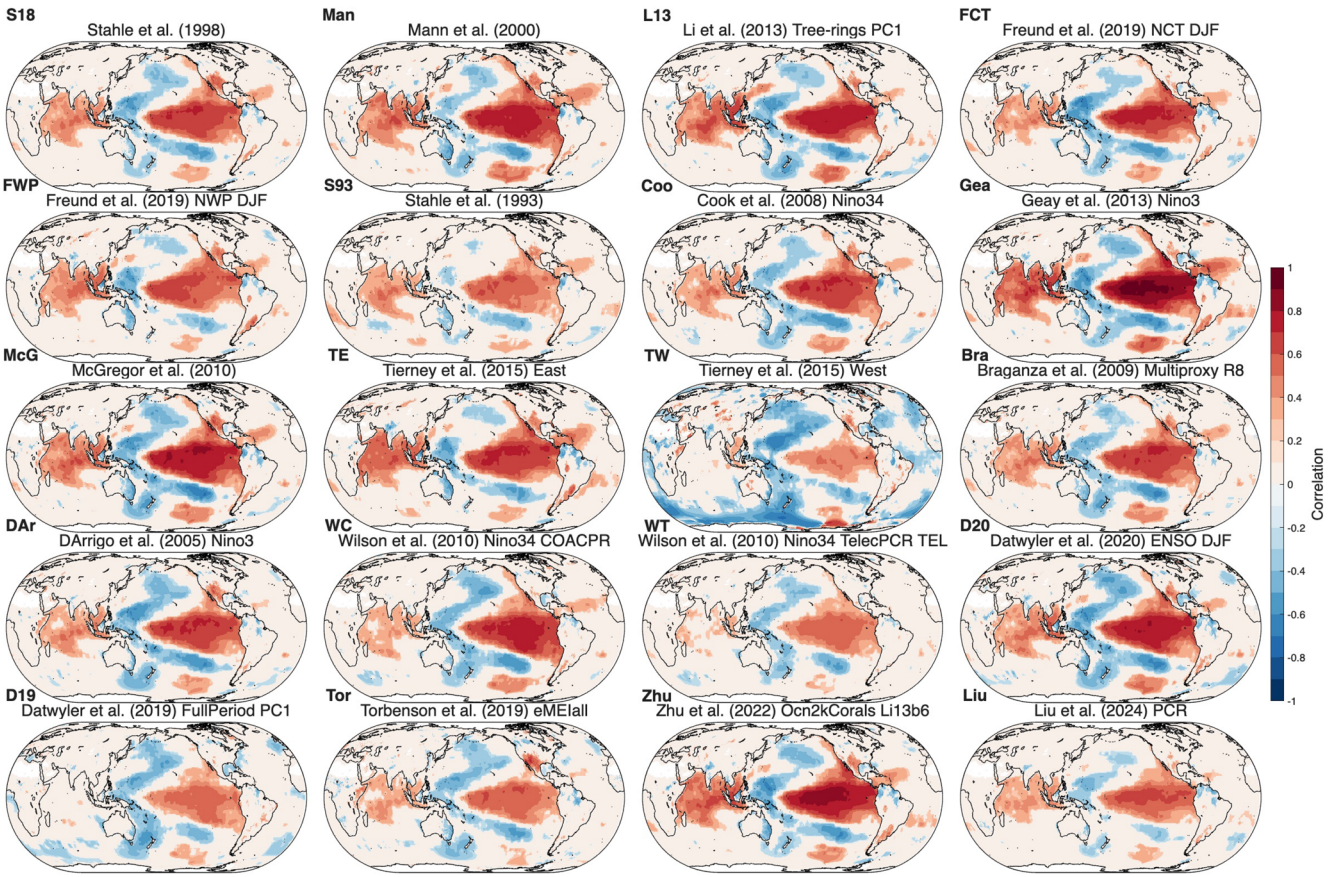


**FIGURE 6** | Spatial signatures Spatial correlation of the selected ENSO reconstructions with PDSI (Barichivich et al. 2021) over land and SSTs (Rayner et al. 2003) over ocean during the common instrumental period (1900–1971). Only significant correlations ($p < 0.01$) are shown.

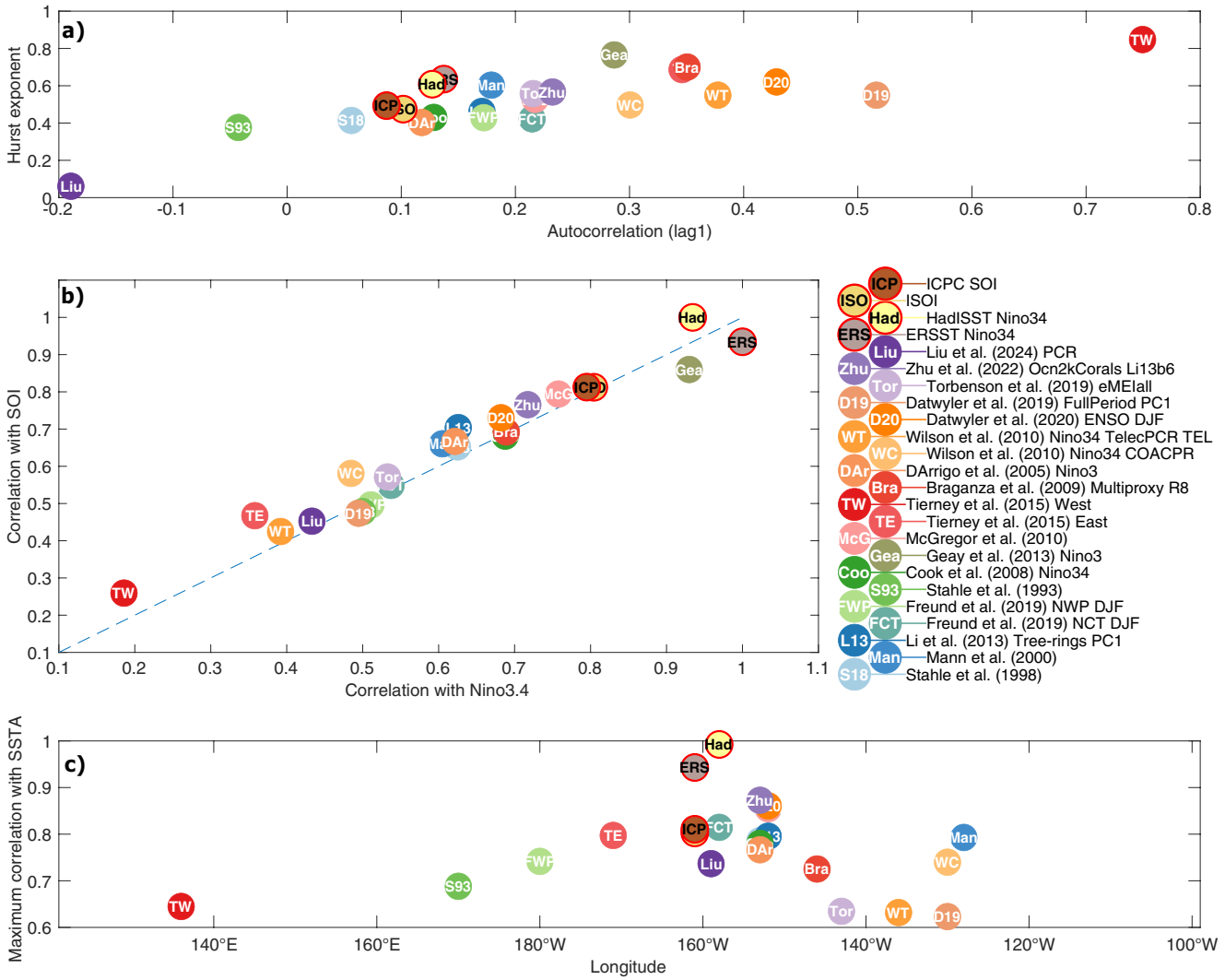


**FIGURE 7** | Characteristics of ENSO reconstructions. (a) Hurst exponent (*y*-axis) and lag-1 autocorrelation (b) Correlation with SOI index (*y*-axis) and Niño3.4 (*x*-axis) and (c), maximum correlation with zonal SSTA ($10^{\circ}N - 10^{\circ}S$) along the equator during instrumental period (1900–1971) of ENSO reconstructions and instrumental data (b).

long-term memory. Many of the reconstructions have similar values, with Gea, Bra, TE and D20 (visually overlapping) all suggesting long-term memory. Several of the reconstructions have less long-term memory than the instrumental data (Liu, S93, S98, DAr, FWP, FCT, Coo), with Liu particularly standing out. The application of a high pass filter in the Liu study (Liu et al. 2024) has clearly influenced long-term memory in that reconstruction. This suggests that the presence of long-term memory is less influenced by the type of proxy used and more by the reconstruction method or preprocessing applied. There is no strong relationship between the Hurst exponent and lag-1 autocorrelation in the reconstructions overall, although both measures are highest in the western Pacific SST reconstruction (Tierney et al. 2015), and lowest in Liu (Liu et al. 2024). The TW reconstruction, which targets the western Pacific and is not specifically an ENSO reconstruction, is also distinct owing to its weak relationship ($r < 0.3$) with the instrumental SOI and Niño3.4 (Figure 7b). The remaining reconstructions exhibit significant moderate-strong correlations ($r = \sim 0.4–0.7$) with both instrumental indices. Leaving aside Gea, for which instrumental data are included for the instrumental period, the strongest correlations with the SOI and Niño3.4 indices occurs for McG and Zhu.

Understanding which longitudinal zone each reconstruction is best related is useful if relying on a single reconstruction to provide a record of past ENSO variability. This may be particularly relevant if considering the impacts of past events. Figure 7c shows the longitude at which the maximum correlation of each reconstruction with the SSTs occurs in the tropical Pacific (10° N–10° S). This maximum signal is spread across a relatively wide swathe of the Pacific (Figure 7c). However, the majority of maximum correlations cluster within the Niño3.4 zone, including those that target Niño3 (Man, DAr). The maximum SST correlations for the WC, WT and D19 reconstructions that target Niño3.4 also fall into the Niño3 zone. Bra (first mode of variability among proxies) and Tor (MEI) also best relate to Niño3.4. The strongest of these maximum longitudinal correlations occur for Zhu and D20 while lowest—but still highly significant—correlations occur for TW, Tor, WT, and D19. TW also stands out because its maximum SST correlation occurs much further west ($\sim 138^{\circ}$ E)than for the remaining reconstructions. Interestingly,

FWP that also represents the western Pacific and utilizes a number of the same proxy records as TW, better represents conditions at ~180° W towards the edge of the Niño3.4 zone. S93 also reflects Central Pacific SST variability close to the Niño4 region. This broad longitudinal range highlights the spatially diverse ENSO signal contained in the reconstructions.

## 5.5 | Time-Dependent Characteristics of ENSO

While cross-correlations (Figure 5) offer a static view of the relationships between paired reconstructions, a moving window comparison of reconstructions against the ensemble mean (the mean of all reconstructions) provides deeper insights into how these relationships evolve over time (Figure 8a). These temporal relationships, estimated using a moving 30-year window, reveal a decreasingly common signal back in time. Divergence among reconstructions is especially apparent between 1600 and 1850 where we have the highest number of reconstructions available (Figure 8). Highest correlations with the ensemble mean are achieved during the instrumental period, and this is consistent with previous findings (Wilson et al. 2010). Most reconstructions (e.g., McG, L13, Tor, Zhu) remain positively correlated with the ensemble mean for their entire length, although some have very weak or even negative correlation back in time (e.g., D20,TW, TE, WT, FWP). There are also some distinct periods over which individual reconstructions depart considerably from the ensemble's mean (e.g., D20). While moving correlation with the reconstruction ensemble mean is not a physically meaningful reference measure of agreement, it does highlight when divergence in the ENSO signal occurs. However, some caution should be applied when considering these moving window correlation results. This is because using the ensemble mean as a baseline has limitations, as apparent shifts in cross-correlations may be the result of different reconstructions covering differing time periods rather than changes in the true relationship.

We can also examine how variance changes over time (Figure 8b). The highest variance for a number of records occurs in the early to mid 20th century, with generally high variance in many reconstructions also occurring around 1800. This may either reflect enhanced ENSO variability at this time or be related to the reconstruction process. The quite strong agreement among records at these times, however, does suggest it is a common feature of ENSO variability similar to (McGregor et al. 2013). Reduced variance exists for many reconstructions in the mid 19th century. As reconstructions drop out back in time, it is increasingly difficult to observe commonalities in variance across reconstructions. In general, a noticeable discrepancy in ENSO variance in the reconstructions is evident throughout the last millennium. One previously identified issue is that inherent uncertainty within climate proxies can lead to an underestimation of the magnitudes of low-frequency variability in some reconstruction methods (Klockmann et al. 2022; Smerdon 2012; von Storch et al. 2004). Dating uncertainties, particularly in the early parts of the ENSO reconstructions where fewer proxy records are available, can affect the representation of its variability. These uncertainties may lead to misalignment of signals

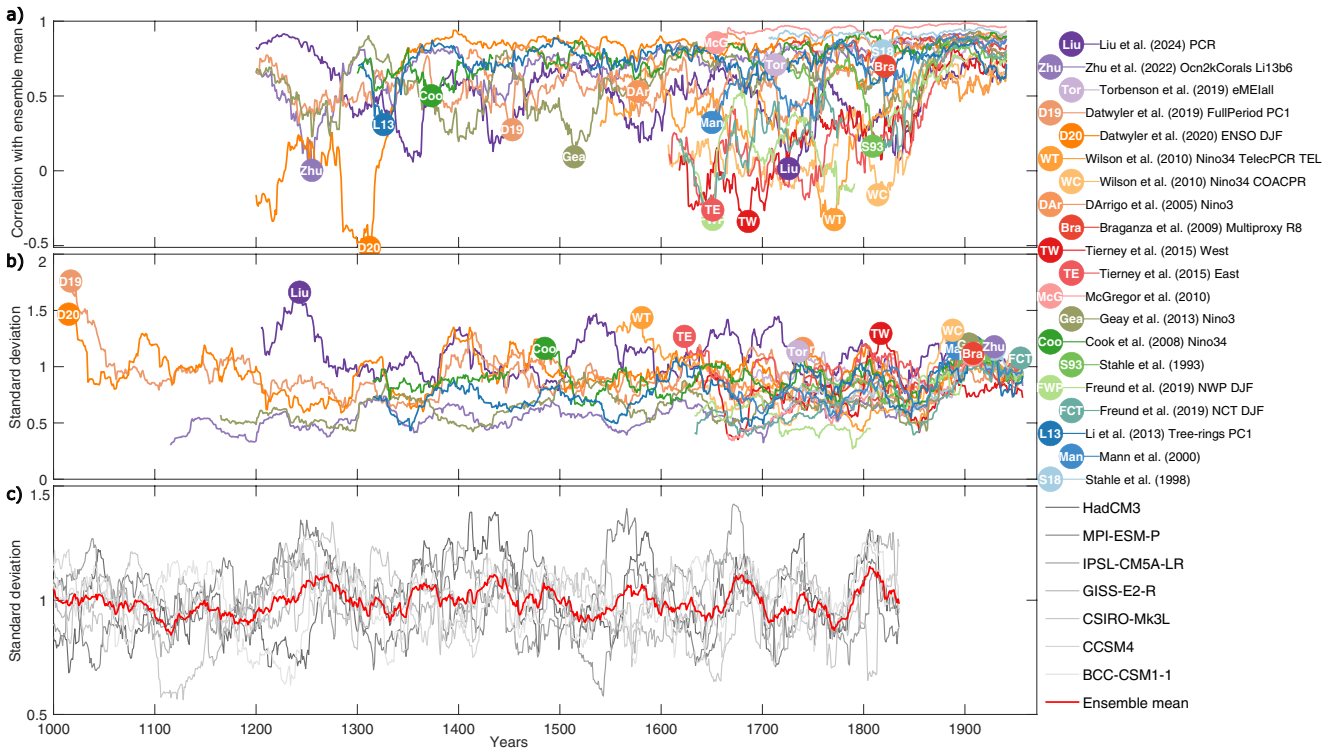


**FIGURE 8** | Time-dependent characteristics of past ENSO (a) Evolution of correlation of ENSO reconstructions with the ensemble mean over 31-year moving windows. Each filled circle indicates the minimum correlation with the ensemble mean for that reconstruction. (b) Evolution of variance in ENSO reconstructions presented by its normalized standard deviation aggregated over 31-year moving windows. Each filled circle indicates the maximum value of its respective reconstruction. (c) Evolution of variance in the Niño3.4 region by palaeoclimate model simulations of the past 1000 years in 31-year moving windows (Brown et al. 2016).

from different proxies, potentially impacting the overall variance depending on the specific nature of the uncertainties and the reconstruction methods used. Pseudo proxy experiments to examine the influence of non-stationary teleconnections (Batehup et al. 2015) and examination of multiple reconstruction techniques (Emile-Geay and Tingley 2015) can provide useful insights for understanding low-frequency behavior of ENSO and confidence in this behavior over time.

The evolution of ENSO variance for a set of available PMIP3 and PMIP4 simulations of the last millennium (Brown et al. 2016) also reveals a degree of consistency between reconstructed and simulated ENSO variance for some periods (Figure 8c). The high variability in the Liu reconstruction (Liu et al. 2024) around 1250 is also simulated by the majority of models as a possible response to strong volcanic eruptions (Lewis and LeGrande 2015). McGregor et al. (2020) and references within showed that the majority of 17 analyzed ENSO reconstructions covering on average 550 years and climate models display a significant eastern Pacific warming in response to volcanic eruptions. Another period of relatively high ENSO variance (activity) in both the reconstructions and models occurs around 1800 (Figure 8b,c). Highest ensemble median variability over the past millennium is observed in the model simulations at this time. Phases of reduced variance in the reconstructions like the mid-late 18th Century and 16th Century are also evident in some climate model simulations (Figure 8c). However, agreement across reconstructions is mixed, and we emphasize that no formal statistical analysis has been conducted here. Periods such as the early 19th century also show increased ENSO variance in both models and some reconstructions, but these apparent similarities should be treated cautiously and warrant further quantitative evaluation in future studies.

For strong agreement at low frequencies, it would be expected that clear low frequency signals would be detectable in, and similar across, the reconstructions. However, this strong low frequency variability is not evident in the frequency domain of the reconstructions over their common period (1727–1971; Figure 9), and this is consistent with the differences observed across most of the last millennium (Figure 8). Lower frequency variability is most evident in TW, TE, D19, D20 and Tor. A lack of low frequency information is most evident in Liu, with FCP, FWP and S93. Instead, the power spectra are dominated by power at the higher frequencies ($> \sim 0.125$, or periods $> \sim 8$ years) and generally persists throughout the reconstructions, even though it is not always significant (Figure 9). The strength of the higher frequency signal in Gea, WC, WT, McG, FWP, and Z22 notably diminishes prior to the instrumental period.

### 5.6 | Insights Into Discrete ENSO Event Reconstructions

A summary of past events from discrete records focusing exclusively on El Niño events is presented in Figure 10a, while Figure 10b, shows a summary of both El Niño and La Niña events. For El Niño events, there is a large degree of overlap between the Quinn and Mayolo (1987) and Garcia-Herrera et al. (2008) records. The overlap and agreement are highest during the 19th century. The relatively high level of disagreement between the records overall, however, means there is considerable uncertainty in the occurrence of events.

Although bias towards a certain type of ENSO has been reported for logbook-based and multi-proxy reconstructions (Barrett et al. 2018), we cannot detect (Figure 10a) any such bias towards EP or CP events in these documentary records identified in the continuous Freund et al. (2019) records, although during the 20th Century, Quinn and Mayolo (1987) CP events seem to be detected less often. None of the mostly CP El Niño events overlap with the (Garcia-Herrera et al. 2008) or (Quinn and Mayolo 1987) El Niño years in the 17th Century. Both records identify strong canonical El Niño events in 1791, 1877, and 1817. Some events common to both records (1618, 1718, and 1884) are documented as likely CP El Niño by Freund et al. (2019).

Similarly, there is no strong evidence of a bias towards either El Niño or La Niña events. The degree of agreement between the Gergis and Fowler (2009) and Brönnimann et al. (2007) is similar to that shown in Figure 10a for El Niño only events, although there is some evidence that agreement varies over time. For example, during the 16th Century, most agreement relates to La Niña years, whereas there is stronger agreement about El Niño years in the 20th Century.

Discrete ENSO event reconstructions provide qualitative evidence of past ENSO activity, but their interpretation is subject to considerable uncertainty, as reflected in disagreements among records. These reconstructions can be regionally biased, may overemphasize extreme events, and may not solely reflect ENSO signals due to teleconnections. Dating can be imprecise, with reconstructions disagreeing on event timing, type, or magnitude, and such discrepancies must be treated with caution given the underlying uncertainties in the historical sources.

## 6 | From Past to Future: Advancing Enso Understanding Through Reconstructions and Modeling

### 6.1 | Climate Model Benchmarking

Documentary evidence (discrete event evidence) and palaeoclimate proxies that are either direct or indirect measures of the atmospheric or oceanic components of the El Niño Southern Oscillation provide important information about ENSO variability over the last millennium. Yet, this palaeo-record of ENSO events and variability is not widely used by the climate modeling community, or in attribution and climate projection studies. The main challenge hindering comparative studies seems to be the disconnect between different fields in accessing and understanding palaeoclimate information. A large number of ENSO reconstructions are yet to be fully exploited, and we suggest that the information from these records should be harnessed by the wider climate community wherever possible. Reference datasets, similar to those used for model evaluations of ENSO (Planton et al. 2021), could be extended to include suitable palaeo-ENSO variability. Not only would this expand the number of ENSO events available for analysis, it would also provide the potential for a more realistic assessment of the extent of multi-decadal variability expressed in instrumental records

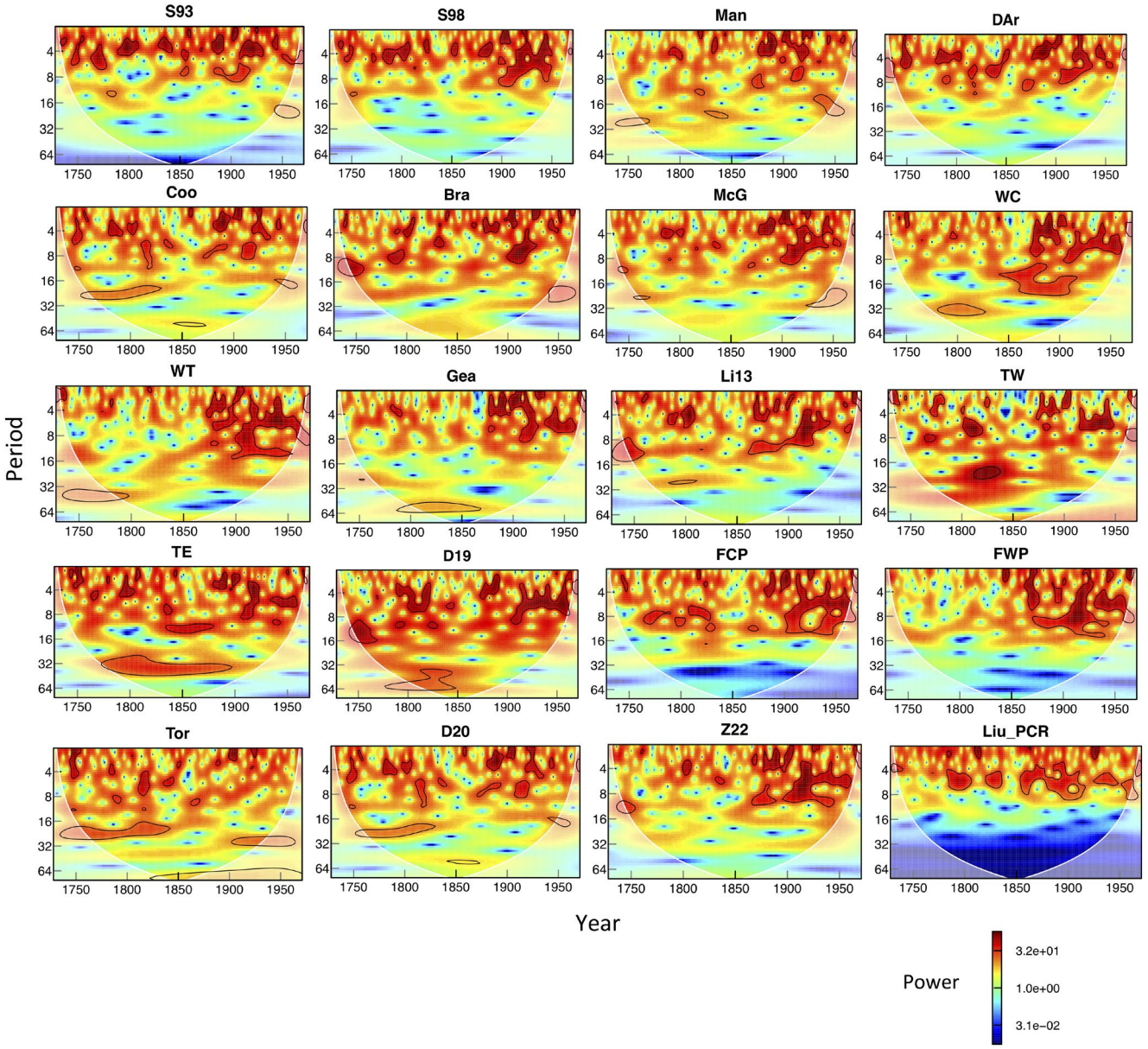


**FIGURE 9** | Wavelets of all selected reconstructions (see Table 1) over their common period, 1727–1971. Note that WC, WT and Gea all use instrumental data for the most recent parts of the reconstructions.

(Dieppois et al. 2021). Making use of palaeo-ENSO records would enable would also enable ENSO behaviors not observed during the past ~50 years of satellite observations to be incorporated into analyses of ENSO including attribution and extreme event studies.

## 6.2 | Differences and Similarities Between Sources of Pre-Industrial ENSO

Several commonalities across ENSO reconstructions can be highlighted, for example, some periods of consistently high or low ENSO variability (Figure 8b), and agreement on the timing of specific events (Figure 11a). Notably, there is some indication from continuous reconstructions that La Niña events were relatively frequent during the 16th and late 19th centuries. Although the number of records is lower prior to 1600 CE, there is still notable agreement on certain individual events during the 15th and 16th centuries. This agreement in high-frequency variability has important implications for understanding past hydroclimate in regions such as the southwestern United States, Central America, northern South America, the Maritime Continent, and eastern Australia (Figure 6).

Despite commonalities, ENSO reconstructions are not flawless extensions of the instrumental record. As clearly shown in Figures 5–10 no two reconstructions are the same, and this applies equally to the discrete and continuous reconstructions. No single ENSO reconstruction captures all important features of ENSO equally well. These differences (Figure 4) stem from a range of factors, including choices made about what archives or proxy selection criteria to use, reconstruction methodology, geographical source regions of proxies (e.g., D20 compared to WC), season targeted (e.g., Jan–Dec (D19) or

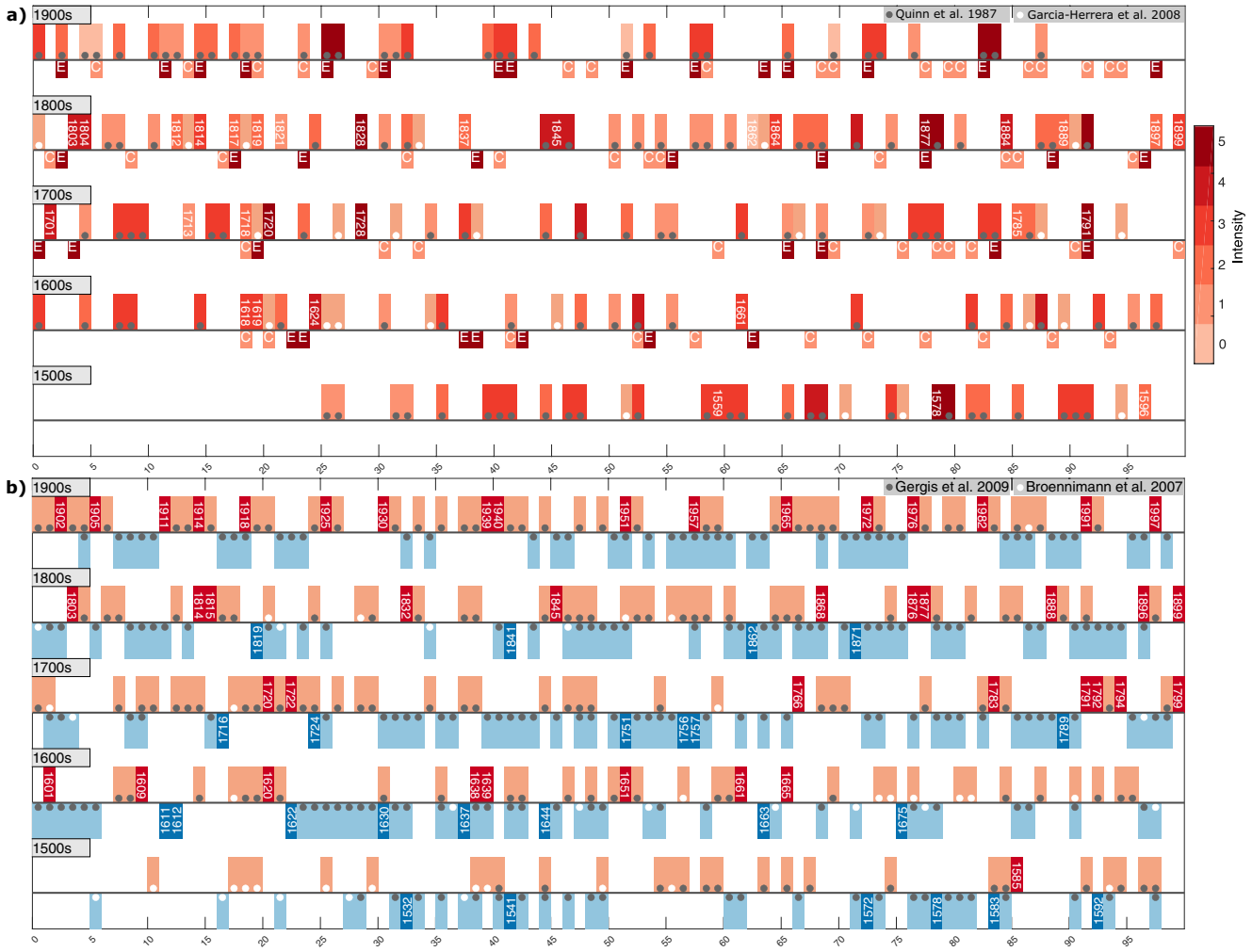


**FIGURE 10** | Discrete ENSO events (a) Past El Niño events as reported by (Quinn and Mayolo 1987) and (Garcia-Herrera et al. 2008). Overlapping years are highlighted by including the year. Possible Eastern (E) and Central (C) Pacific El Niño events are indicated according to (Freund et al. 2019). (b) Discrete El Niño and La Niña events identified by Gergis and Fowler (2009) and Brönnimann et al. (2007). Overlapping years are highlighted by color and year for El Niño events (red) and La Niña events (blue).

DJF), and instrumental ENSO index or indices reconstructed (e.g., SOI (S93) or Ninño3.4 (Gea)). One issue that may also be relevant here is the 'no-analogue issue.' This can arise when the instrumental record, against which a reconstruction is calibrated, does not include values as extreme as those suggested by the proxy records outside the calibration period, or when the period used for calibration is, for example, much more La Niña-like compared to the rest of the reconstructed period. This is essentially an extrapolation issue and its impact will likely differ across the different palaeo-records incorporated into a reconstruction and be influenced by reconstruction methodology. Understanding its potential influence on pre-instrumental differences among reconstructions would require detailed investigation.

Another key reason for differences may arise from the geographical location of proxies that can significantly influence how well a reconstruction represents variability in different sectors of the Pacific (Stevenson et al. 2013), or teleconnections associated with hydroclimate in different regions (Figure 6). Coral records located in the centre of action are directly influenced by the equatorial cold tongue in the eastern/central Pacific, while coral records from locations directly influenced by the SPCZ or from the western Pacific warm pool better represent those areas. Selecting a reconstruction or subset of reconstructions that best represents the desired ENSO characteristics (e.g., season, index, centre-of-action or teleconnected signal) requires some a priori knowledge of ENSO variability.

Chronological uncertainties are a fundamental challenge in interpreting reconstructed ENSO variability. In layer-counted archives like annually banded corals, slight misalignments in growth increments can blur interannual climate signals and reduce the reconstructed amplitude of individual El Niño or La Niña events. These dating imprecisions grow more pronounced in older fossil coral samples that lack overlap with instrumental records. Combining multiple proxy types can help to randomize individual age offsets and preserve dominant ENSO features, but as proxy density thins back in time, the influence of chronological errors on reconstruction fidelity inevitably increases.

Recent developments in probabilistic age modeling and uncertainty quantification provide a path forward. (Comboul

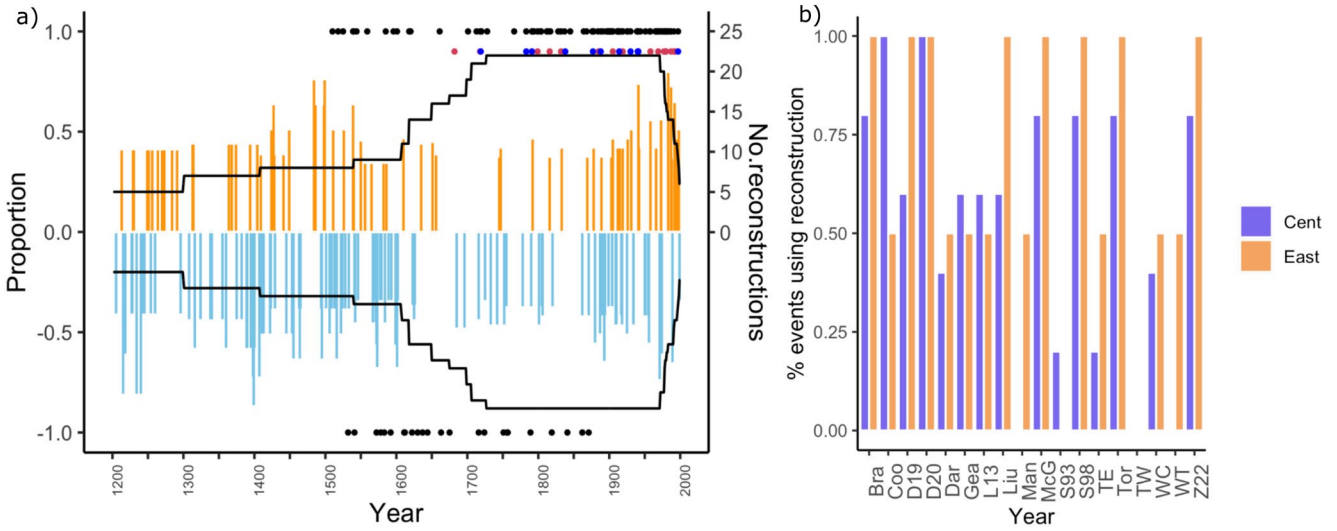


**FIGURE 11** | (a) Palaeo-ENSO events through time, based on agreement among records. Continuous reconstructions are shown as bars, orange represents El Niño events, and blue, La Niña events. Only events for which at least 33% of reconstructions agree are shown. Thresholds of ±0.8 (Niño indices) and of ±8 (SOI) were applied to identify events. Black dots show events where at least 2/3 of the four discrete event reconstructions (El Niño) or both the two reconstructions (La Niña) agree an event occurred. The blue and red dots show the occurrence of EP or CP events identified by Freund et al. (2019). Dashed lines show the period over which the documentary records used, or the FCT and FWP records extend. (b) The proportion of EP and CP events identified in the FCT and FWP reconstructions also detected by other selected continuous reconstructions.

et al. 2014) explores Bayesian frameworks for corals that explicitly address missing and double-counted growth increments, revealing how error rates translate into high-frequency and decadal signal distortions. Extended spectral uncertainty analysis across proxy types can potentially highlight systematic biases that standard calibrations overlook (Dolman et al. 2021). Furthermore, the advantages of integrated probabilistic approaches in correcting chronological errors during proxy calibration could lead to further improvements (Dee et al. 2015; Dolman et al. 2021). Some propagating age uncertainties could potentially be mitigated by smoothing individual records prior to index calculation and shifting targets from seasonally and annually resolved anomalies towards decadal variance or extreme-event counts. Such strategies, coupled with ensemble-based reconstructions and rigorous age-model diagnostics, will strengthen confidence in the temporal evolution of ENSO variability, particularly for deeper-time intervals.

Overall, based on our comparison of interannual ENSO reconstructions, it is difficult to make clear and unambiguous conclusions about general trends in ENSO's evolution over the past millennium, precise timing of events, or some characteristics in the frequency domain (Lu et al. 2018). However, as is the case with climate simulations, these differences do not diminish their value. As observed previously (e.g., Wilson et al. 2010), all the reconstructions exhibit ENSO sensitivity, capturing some aspects of its occurrence (also see Figure 7). To gain a more comprehensive understanding of past ENSO activity, a promising approach is to integrate multiple lines of evidence, utilizing ensembles of palaeo-ENSO reconstructions. This strategy may prove to be the most effective way to incorporate palaeo-ENSO knowledge into model evaluation and projection studies, offering a richer, more nuanced perspective on ENSO variability through time.

### 6.3 | The Future—Ensemble Reconstructions to Better Reveal the ENSO Spectrum?

Differences among the reconstructions present a range of important opportunities for further research. These opportunities are not unlike those met by the global climate modeling (GCM) community and their data users. GCM output (and regional climate models) vary greatly; however, the community has identified standard methods and approaches to deal with the range of outcomes/uncertainty in the future projections. The palaeoclimate community can take valuable lessons from this approach to utilize multiple ENSO reconstructions and combine these with the palaeo GCM ENSO simulations. We can also draw important conclusions from similarities in variability changes in the reconstructions, or from agreement in identified events (Figures 8b and 11a). These similarities among reconstructions may provide greater confidence around past ENSO activity in some periods, such as the 17th and 18th centuries (Figure 10). Similarly, it has been shown that inclusion of records from regions peripheral to ENSO's main impacts can add significantly to the reconstruction skill (Evans et al. 2000; Freund et al. 2019). The use of records from these regions can allow for an assessment of temporal differences between reconstructions based mostly, or solely, on proxies from the central Pacific and those relying on teleconnected signals. Such analysis may assist with analyses of the temporal stability and strength of teleconnections over time. As another example, reconstructions targeting the SST-based Niño indices may display different behavior for some time periods compared to SLP reconstructions (i.e., those targeting the SOI or the Walker cell). Therefore, the availability of a variety of reconstructions may facilitate investigations of decoupling of the oceanic and atmospheric components of ENSO over long time frames (Hu et al. 2020). Different ENSO reconstructions rely on various proxy types, each with its own

strengths and limitations. Tree-rings, for instance, offer the least risk of significant dating uncertainties due to their annual banding and typically large sample sizes, which allow for cross-dating records (Emile-Geay et al. 2020). However, tree-rings often provide indirect measures of ENSO through teleconnections. In contrast, coral archives offer more direct ENSO measurements but come with some degree of dating uncertainty. Living corals can provide precise relative and absolute dating, though they are often not as well-replicated as tree-ring records (Dee et al. 2015). Fossil coral records, while valuable, may be influenced by diagenesis (McGregor and Abram 2008; Stevenson et al. 2013), biological mediation, or misidentification of annual bands. For example, the Palmyra coral record (Cobb et al. 2013) may be less precisely dated and potentially introduce errors (Comboul et al. 2014). It is crucial to consider the proxy type, methods employed, and the level of certainty associated with each reconstruction to ensure robust ENSO analyses.

Our understanding of ENSO's complex spatio-temporal characteristics remains limited but is crucial for assessing future anthropogenic global warming scenarios. While some palaeoclimate studies attempt to discern spatial diversity in the expression of ENSO into two categories (Freund et al. 2019; Grothe et al. 2020), ENSO is actually much more complex (Timmermann et al. 2018). In this vein, exploiting information in the range of existing, and future, ENSO reconstructions may help improve our understanding of ENSO diversity. For example, some reconstructions may provide more information about past occurrence of EP or CP events. Our preliminary—and tentative—example (Figure 11b) may be a useful starting point for considering what information about diversity could be targeted in new, or derived from previous, reconstructions. The example is tentative because we use what is currently the sole explicit reconstruction of EP and CP events that, like all other reconstructions, will have its strengths and weaknesses. Age uncertainties in coral records for example have a stronger impact on the detection of CP events than EP events (Freund et al. 2019). The location of coral proxy records is also often biased towards the western and central Pacific which may result in an underestimation of the amplitude of EP events (Emile-Geay et al. 2020). Additionally, identification of ENSO events in the reconstructions relies on the threshold selected for their identification. In this case, we have used stricter thresholds of ±0.8 for the Niño indices and ±8 for the SOI (Figure 11b) as opposed to ±0.5 and ±7. Based on our analysis (Figure 11b), Man (targeting Niño3) and WT (targeting Niño3.4) detect EPs, but not CPs and Coo (targeting Niño3.4) is more tuned to central Pacific events. Conversely, D20 identifies all EP and all CP events while TW detects neither. Use of lower thresholds for event identification, however, suggests that most reconstructions appear less able to distinguish between EP and CP events. It does appear, however, that some reconstructions are less likely to pick up either EPs or CPs (e.g., S93), while others pick up the majority of both EPs and CPs (e.g., Coo, D20). Another possibility for discerning EP and CP events may be to exploit the location of proxy records utilized in reconstructions. It has been shown that coral records from off-equatorial regions like the SPCZ are more sensitive to CP ENSO events (Stevenson, McGregor, Phipps, & Fox-Kemper 2013).

Combining documentary (discrete) records that are directly related to impacts and continuous reconstructions also offers an opportunity to develop a comprehensive picture of past ENSO events as well as their spatial impacts. This, combined with an improved understanding of past diversity, could be especially useful in considering likely impacts of projected changes in ENSO. Combining multiple documentary records with continuous ENSO information (Gergis and Fowler 2009) provides an opportunity to investigate this further.

Extending the focus beyond SOI and SST-based past ENSO reconstructions, Walker circulation reconstructions like that by (Falster et al. 2023) could provide an opportunity to explore the upper atmospheric dynamics of ENSO variability. As a representation of large-scale equatorial zonal circulation, the Walker circulation offers a complementary perspective on how ENSO events influence and are influenced by atmospheric dynamics. Comparing reconstructed equatorial SLP gradients with the ENSO reconstruction could offer valuable insights into the coupling between oceanic and atmospheric components of tropical climate variability and help assess the coherence and phase relationships between SST anomalies and atmospheric circulation over longer timescales.

The development of improved statistical methods to combine multiple lines of evidence, advances in palaeoclimate data assimilation (Hakim et al. 2016; Tardif et al. 2019), deep learning algorithms (e.g., Wang et al. 2023; Zhang et al. 2022) and large ensembles (Maher et al. 2022) will also help to overcome some of the difficulties palaeoclimate ENSO research has faced. Our increasing appreciation of the multi-faceted ENSO phenomenon requires novel strategies to expand on existing palaeoclimate efforts and help guide future research.

## 7 | Conclusions

Instrumental observations are insufficient for characterizing ENSO beyond the past ~150 years because they cannot capture the full range of natural variability, leaving major uncertainties in how ENSO amplitude, frequency, and diversity evolve on centennial to millennial timescales. Reconstructions extending back through the last millennium are therefore invaluable for capturing the full spectrum of ENSO behavior, for providing independent benchmarks against which climate models can be evaluated and for their potential insight into possible driving mechanisms. This enhanced understanding is vital for validating and constraining climate models that are used for developing future projections of ENSO evolution under anthropogenic climate change. However, the wide variety of ENSO reconstructions now available that have been developed from different proxy data means it is timely to review their similarities, differences, and limitations. Our review has aimed to synthesize what these reconstructions can collectively reveal about ENSO's past variability and dynamics.

To more fully appreciate the continuum of ENSO event types and their manifestation, it will be increasingly crucial to draw on a range of evidence, including long palaeo-ENSO records such as those explored here. These records have a higher chance of capturing the fuller spectrum of ENSO variability.

Our synthesis highlights several robust features across reconstructions. First, ENSO expresses substantial variability on interannual to multidecadal timescales, with evidence for both persistent low-frequency modulation and periods of reduced or enhanced variance. These features are broadly consistent with dynamical expectations and are sometimes reproduced in climate model simulations, though important discrepancies remain. Second, reconstructions diverge in the strength and spatial expression of teleconnections, particularly in their relationships with Indian Ocean SSTs and land-based drought patterns, indicating that ENSO's global impacts are neither stationary nor uniform across records. Third, the location of maximum tropical Pacific SST relationships varies across reconstructions, with some aligning with the Niño3.4 region, while others show stronger connections to central or western Pacific SSTs. This points to potential shifts in ENSO "flavor" and diversity over the last millennium.

Other features that emerge from our review are that the similarity among reconstructions is likely associated with their use of particular types of proxies utilized and the geographical location of these proxies (e.g., center-of-action proxies versus those from the eastern equatorial Pacific). Stronger relationships among reconstructions over the post-1850 period compared to the pre-industrial period are likely due to very strong relationships among the Niño indices in the instrumental period against which the reconstructions have been calibrated. There are differences in their spatial teleconnection signatures, particularly in their relationships with Indian Ocean SSTs and drought patterns over land areas. There is also evidence of long-term persistence and low-frequency variability in some reconstructions similar to instrumental ENSO indices, though the strength of this low-frequency behavior differs among reconstructions. Most relate most strongly to the Niño3.4 region. Reconstructed ENSO variance shows some consistent periods of high and low variance across multiple reconstructions and models over the last millennium (Karamperidou and DiNezio 2022), but there are also notable discrepancies (S. McGregor et al. 2013). Wavelet analyses reveal differences in the strength of low-frequency variability captured by different reconstructions.

Model simulations of the last millennium provide an important counterpart to reconstructions. While there is some apparent overlap between simulated and reconstructed periods of high and low variance, stronger agreement emerges in their common response to large volcanic eruptions, consistent with earlier studies (e.g., Lewis and LeGrande 2015). Models also highlight the role of background climate state and forcing in modulating ENSO amplitude, offering testable hypotheses for palaeo-records. However, statistical coherence between proxy-based reconstructions and models weakens prior to the instrumental period, underscoring the need for more systematic comparison. In particular, there is a decreasing coherence among reconstructions extending back in time, with some reconstructions diverging considerably from the ensemble mean during certain periods. This likely relates to the decreasing number of proxy records available back in time, highlighting a need to target the development of new high-resolution proxy records that extend further back in time and are strategically located in regions sensitive to different ENSO flavors and teleconnections.

Taken together, our analysis underscores the fact that no single reconstruction fully captures the complexity of ENSO. Each dataset has distinct strengths and limitations depending on proxy type, calibration method, and spatial sensitivity. To move forward, we recommend the development of palaeo-ENSO reconstruction ensembles—frameworks that combine multiple records in a way analogous to climate model ensembles. Such ensembles would enable quantification of uncertainties, highlight robust common signals in the pre-Industrial period. Alongside the highly detailed analysis afforded through instrumental data and those available through modeling, these ensembles have the potential to provide a more holistic picture of ENSO's temporal and spatial variability. Ensemble approaches could also be designed to target specific aspects of ENSO behavior (e.g., event diversity, teleconnection stability, or low-frequency modulation), thereby improving model evaluation and enhancing our capacity to anticipate ENSO's future evolution under anthropogenic forcing.

It is important to note that while our review focuses on the last millennium, this period represents a time of relatively small changes in climate forcing compared to earlier epochs. Modeling studies suggest that ENSO variability may have experienced much larger changes during the Holocene (Lawman et al. 2022) and even more substantial shifts during glacial–interglacial transitions (Thirumalai et al. 2024). However, the abundance of high-resolution proxy records for the last millennium has made it a prime target for ENSO reconstruction efforts, as evidenced by the wealth of studies reviewed here. Future work should aim to extend our understanding of ENSO variability further back in time (Liu et al. 2014; Moy et al. 2002; Tudhope et al. 2001), targeting periods of more significant climate forcing changes. This will require developing new proxy records capable of capturing ENSO signals over longer timescales. Additionally, we encourage the modeling community to run more experiments under a wider range of palaeoclimate scenarios, which could provide valuable insights into ENSO's sensitivity to different forcing regimes and help bridge the gap between modern observations and palaeoclimate records.

Ultimately, capitalizing on all sources of relevant information including palaeo-data has the potential to advance our comprehension of the ENSO phenomenon. This is critical for understanding ENSO's role in past and future climate variability. We suggest that advances will come not from relying solely on instrumental or model data, but from integrating long-term palaeo-records, climate model simulations, and targeted ensemble frameworks to more fully capture ENSO's complexity and its influence on global climate. We consider the development and use of palaeo-ENSO reconstruction ensembles as an important path forward to enhance our ability to predict and understand ENSO's role in future climate scenarios.

### Author Contributions

**Mandy B. Freund:** conceptualization (lead), methodology (equal), visualization (equal), writing – original draft (equal), writing – review and editing (equal). **Danielle C. Verdon-Kidd:** conceptualization (equal), methodology (equal), visualization (equal), writing – original draft (equal), writing – review and editing (equal). **Kathryn J. Allen:** conceptualization (equal), methodology (equal), visualization (equal),

writing – original draft (equal), writing – review and editing (equal). **Josephine R. Brown:** methodology (equal), writing – original draft (equal), writing – review and editing (equal).


### Acknowledgments

K.A. was supported by Australian Research Council grant FT200100102. M.B.F. and J.R.B. received support from Australian Research Council grant CE230100012. D.V.K. was supported by the Australian Research Council Discovery Project DP230101868.


### Conflicts of Interest

The authors declare no conflicts of interest.

### Data Availability Statement

Data sharing is not applicable to this article as no new data were created or analyzed in this study.

### Related WIREs Articles

North American megadroughts in the Common Era: reconstructions and simulations

A review of ENSO teleconnections at present and under future global warming

### References


Abram, N. J., N. M. Wright, B. Ellis, B. C. Dixon, J. B. Wurtzel, and M. H. England. 2020. "Coupling of Indo-Pacific Climate Variability Over the Last Millennium." *Nature* 579, no. 7799: 385–392.

Adams, J. B., M. E. Mann, and C. M. Ammann. 2003. "Proxy Evidence for an El Niño-Like Response to Volcanic Forcing." *Nature* 426, no. 6964: 274–278. https://doi.org/10.1038/nature02101.

Alexander, M. A., I. Bladé, M. Newman, J. R. Lanzante, N.-C. Lau, and J. D. Scott. 2002. "The Atmospheric Bridge: The Influence of ENSO Teleconnections on Air–Sea Interaction Over the Global Oceans." *Journal of Climate* 15, no. 16: 2205–2231. https://doi.org/10.1175/1520-0442(2002)015<2205:tabtio>2.0.co;2.

Alizadeh, O. 2024. "A Review of Enso Teleconnections at Present and Under Future Global Warming." *Wiley Interdisciplinary Reviews: Climate Change* 15, no. 1: e861.

Allan, R., J. Lindesay, and D. Parker. 1996. *El Niño Southern Oscillation & Climatic Variability*. CSIRO Publishing.

Allan, R., N. Nicholls, and P. Jones. 1991. "A Further Extension of the Tahiti-Darwin SOI, Early ENSO Events and Darwin Pressure." *Journal of Climate* 4: 743–749.

Allan, R. J. 1988. "El Niño Southern Oscillation Influences in the Australasian Region." *Progress in Physical Geography* 12, no. 3: 313–348.

Allan, R. J. 2000. *Enso and Climatic Variability in the Last 150 Years*. Cambridge University Press.

Allen, R. J., and R. G. Anderson. 2018. "21st Century California Drought Risk Linked to Model Fidelity of the El Niño Teleconnection." *npj Climate and Atmospheric Science* 1, no. 1: 21. https://doi.org/10.1038/s41612-018-0032-x.

Ashok, K., S. K. Behera, S. A. Rao, H. Weng, and T. Yamagata. 2007. "El Niño Modoki and Its Possible Teleconnection." *Journal of Geophysical Research* 112, no. C11: C11007.

Ashok, K., and T. Yamagata. 2009. "Climate Change: The El Niño With a Difference." *Nature* 461, no. 7263: 481–484.

Barichivich, J., T. Osborn, I. Harris, G. van der Schrier, and P. Jones. 2021. "Monitoring Global Drought Using the Self-Calibrating Palmer Drought Severity Index." In *Bulletin of the American Meteorological Society*, edited by R. Dunn, F. Aldred, N. Gobron, J. Miller, and K. Willett, vol. 102, S68–S70. AMS.

Barnston, A. G., M. Chelliah, and S. B. Goldenberg. 1997. "Documentation of a Highly Enso-Related Sst Region in the Equatorial Pacific." *Atmosphere–Ocean (Canadian Meteorological & Oceanographic Society)* 35, no. 3: 367.

Barrett, H. G., J. M. Jones, and G. R. Bigg. 2018. "Reconstructing El Niño Southern Oscillation Using Data From Ships Logbooks, 1815–1854. Part ii: Comparisons With Existing Enso Reconstructions and Implications for Reconstructing Enso Diversity." *Climate Dynamics* 50: 3131–3152.

Batehup, R., S. McGregor, and A. J. E. Gallant. 2015. "The Influence of Non-Stationary Teleconnections on Palaeoclimate Reconstructions of ENSO Variance Using a Pseudoproxy Framework." *Climate of the Past* 11, no. 12: 1733–1749. https://doi.org/10.5194/cp-11-1733-2015.

Bertrand, A., M. Lengaigne, K. Takahashi, A. Avadi, F. Poulain, and C. Harrod. 2020. *El Niño Southern Oscillation (Enso) Effects on Fisheries and Aquaculture*. Vol. 660. Food & Agriculture Org.

Bjerknes, J. 1969. "Atmospheric Teleconnections From the Equatorial Pacific." *Journal of the Atmospheric Sciences* 97, no. 3: 163–172.

Braconnot, P., S. P. Harrison, M. Kageyama, et al. 2012. "Evaluation of Climate Models Using Palaeoclimatic Data." *Nature Climate Change* 2, no. 6: 417–424.

Bradley, R. S., and P. D. Jonest. 1993. "'Little Ice Age' Summer Temperature Variations: Their Nature and Relevance to Recent Global Warming Trends." *Holocene* 3, no. 4: 367–376. https://doi.org/10.1177/095968369300300409.

Brady, E., S. Stevenson, D. Bailey, et al. 2019. "The Connected Isotopic Water Cycle in the Community Earth System Model Version 1." *Journal of Advances in Modeling Earth Systems* 11, no. 8: 2547–2566. https://doi.org/10.1029/2019MS001663.

Braganza, K., J. L. Gergis, S. B. Power, J. S. Risbey, and A. M. Fowler. 2009. "A Multiproxy Index of the El Niño–Southern Oscillation, A.D. 1525–1982." *Journal of Geophysical Research* 114, no. D5: D05106–D05117.

Brönnimann, S., E. Xoplaki, C. Casty, A. Pauling, and J. Luterbacher. 2007. "Enso Influence on Europe During the Last Centuries." *Climate Dynamics* 28: 181–197.

Brown, J. R., C. M. Brierley, S.-I. An, et al. 2020. "Comparison of Past and Future Simulations of ENSO in CMIP5/PMIP3 and CMIP6/PMIP4 Models." *Climate of the Past* 16, no. 5: 1777–1805. https://doi.org/10.5194/cp-16-1777-2020.

Brown, J. R., P. Hope, J. Gergis, and B. J. Henley. 2016. "ENSO Teleconnections With Australian Rainfall in Coupled Model Simulations of the Last Millennium." *Climate Dynamics* 47: 79–93.

Buhler, J. C., J. Axelsson, F. A. Lechleitner, et al. 2022. "Investigating Stable Oxygen and Carbon Isotopic Variability in Speleothem Records Over the Last Millennium Using Multiple Isotope-Enabled Climate Models." *Climate of the Past* 18, no. 7: 1625–1654. https://doi.org/10.5194/cp-18-1625-2022.

Cai, W., B. Ng, T. Geng, et al. 2023. "Anthropogenic Impacts on Twentieth-Century ENSO Variability Changes." *Nature Reviews Earth & Environment* 4, no. 6: 407–418. https://doi.org/10.1038/s43017-023-00427-8.

Cai, W., P. v. Rensch, T. Cowan, and A. Sullivan. 2010. "Asymmetry in ENSO Teleconnection With Regional Rainfall, Its Multidecadal Variability, and Impact." *Journal of Climate* 23, no. 18: 4944–4955. https://doi.org/10.1175/2010jcli3501.1.

Cai, W., A. Santoso, M. Collins, et al. 2021. "Changing El Niño–Southern Oscillation in a Warming Climate." *Nature Reviews Earth & Environment* 2, no. 9: 628–644.

Cai, W., A. Santoso, G. Wang, et al. 2015. "ENSO and Greenhouse Warming." *Nature Climate Change* 5, no. 9: 849–859. https://doi.org/10.1038/nclimate2743.

Cai, W., A. Santoso, G. Wang, et al. 2020. "ENSO Response to Greenhouse Forcing." In *El Niño Southern Oscillation in a Changing Climate*, vol. 13, 289–307. American Geophysical Union.

Cai, W., G. Wang, B. Dewitte, et al. 2018. "Increased Variability of Eastern Pacific El Niño Under Greenhouse Warming." *Nature* 564, no. 7735: 201–206. https://doi.org/10.1038/s41586-018-0776-9.

Cai, W., L. Wu, M. Lengaigne, et al. 2019. "Pantropical Climate Interactions." *Science* 363, no. 6430: eaav4236. https://doi.org/10.1126/science.aav4236.

Capotondi, A., S. McGregor, M. J. McPhaden, et al. 2023. "Mechanisms of Tropical Pacific Decadal Variability." *Nature Reviews Earth & Environment* 4, no. 11: 754–769. https://doi.org/10.1038/s43017-023-00486-x.

Capotondi, A., A. T. Wittenberg, M. Newman, et al. 2015. "Understanding ENSO Diversity." *Bulletin of the American Meteorological Society* 96, no. 6: 921–938. https://doi.org/10.1175/bams-d-13-00117.1.

Chen, C., M. A. Cane, A. T. Wittenberg, and D. Chen. 2016. "ENSO in the CMIP5 Simulations: Lifecycles, Diversity, and Responses to Climate Change." *Journal of Climate* 30, no. 2: 775–801. https://doi.org/10.1175/jcli-d-15-0901.1.

Chiang, J. C. H., and D. J. Vimont. 2004. "Analogous Pacific and Atlantic Meridional Modes of Tropical Atmosphere–Ocean Variability*." *Journal of Climate* 17, no. 21: 4143–4158. https://doi.org/10.1175/jcli4953.1.

Chung, P.-H., and T. Li. 2013. "Interdecadal Relationship Between the Mean State and El Niño Types*." *Journal of Climate* 26, no. 2: 361–379. https://doi.org/10.1175/jcli-d-12-00106.1.

Cobb, K. M., C. D. Charles, H. Cheng, and R. L. Edwards. 2003. "El Niño/Southern Oscillation and Tropical Pacific Climate During the Last Millennium." *Nature* 424, no. 6946: 271–276.

Cobb, K. M., N. Westphal, H. R. Sayani, et al. 2013. "Highly Variable El Nino-Southern Oscillation Throughout the Holocene." *Science* 339, no. 6115: 67–70. https://doi.org/10.1126/science.1228246.

Comboul, M., J. Emile-Geay, M. N. Evans, N. Mirnateghi, K. M. Cobb, and D. M. Thompson. 2014. "A Probabilistic Model of Chronological Errors in Layer-Counted Climate Proxies: Applications to Annually Banded Coral Archives." *Climate of the Past* 10, no. 2: 825–841. https://doi.org/10.5194/cp-10-825-2014.

Cook, E. R., R. D. D'Arrigo, and K. J. Anchukaitis. 2008. "ENSO Reconstructions from Long Tree-Ring Chronologies: Unifying the Differences? Talk Presented at a Special Workshop on "Reconciling ENSO Chronologies for the Past 500 Years", Held in Moorea, French Polynesia on April 2–3, 2008."

Corringham, T. W., and D. R. Cayan. 2019. "The Effect of El Niño on Flood Damages in the Western United States." *Weather, Climate, and Society* 11, no. 3: 489–504.

D'Arrigo, R., E. Cook, R. Villalba, et al. 2000. "Trans-Tasman Sea Climate Variability Since AD 1740 Inferred From Middle to High Latitude Tree-Ring Data." *Climate Dynamics* 16, no. 8: 603–610.

D'Arrigo, R., E. R. Cook, R. J. Wilson, R. Allan, and M. E. Mann. 2005. "On the Variability of Enso Over the Past Six Centuries." *Geophysical Research Letters* 32, no. 3: L03711.

Dasgupta, P., M. Roxy, R. Chattopadhyay, C. Naidu, and A. Metya. 2021. "Interannual Variability of the Frequency of Mjo Phases and Its Association With Two Types of Enso." *Scientific Reports* 11, no. 1: 11541.

Dätwyler, C., N. J. Abram, M. Grosjean, E. R. Wahl, and R. Neukom. 2019. "El Niño–Southern Oscillation Variability, Teleconnection Changes and Responses to Large Volcanic Eruptions Since AD 1000." *International Journal of Climatology* 39, no. 5: 2711–2724. https://doi.org/10.1002/joc.5983.

Dätwyler, C., M. Grosjean, N. J. Steiger, and R. Neukom. 2020. "Teleconnections and Relationship Between the El Niño–Southern Oscillation (Enso) and the Southern Annular Mode (Sam) in Reconstructions and Models Over the Past Millennium." *Climate of the Past* 16, no. 2: 743–756.

Dayem, K. E., D. C. Noone, and P. Molnar. 2007. "Tropical Western Pacific Warm Pool and Maritime Continent Precipitation Rates and Their Contrasting Relationships With the Walker Circulation." *Journal of Geophysical Research* 112, no. D6: 2007–2012.

Dee, S., J. Emile-Geay, M. N. Evans, A. Allam, E. J. Steig, and D. Thompson. 2015. "PRYSM: An Open-Source Framework for PRoxY System Modeling, With Applications to Oxygen-Isotope Systems." *Journal of Advances in Modeling Earth Systems* 7, no. 3: 1220–1247. https://doi.org/10.1002/2015ms000447.

Dee, S. G., K. M. Cobb, J. Emile-Geay, et al. 2020. "No Consistent Enso Response to Volcanic Forcing Over the Last Millennium." *Science* 367, no. 6485: 1477–1481.

DeLong, K. L., T. M. Quinn, F. W. Taylor, K. Lin, and C.-C. Shen. 2012. "Sea Surface Temperature Variability in the Southwest Tropical Pacific Since AD 1649." *Nature Climate Change* 2, no. 11: 799–804.

DeLong, K. L., T. M. Quinn, F. W. Taylor, C.-C. Shen, and K. Lin. 2013. "Improving Coral-Base Paleoclimate Reconstructions by Replicating 350years of Coral Sr/ca Variations." *Palaeogeography, Palaeoclimatology, Palaeoecology* 373: 6–24. https://doi.org/10.1016/j.palaeo.2012.08.019.

Diamond, M. S., and R. Bennartz. 2015. "Occurrence and Trends of Eastern and Central Pacific El Niño in Different Reconstructed SST Data Sets." *Geophysical Research Letters* 42, no. 23: 10,375–10,381. https://doi.org/10.1002/2015gl066469.

Diaz, H. F., and V. Markgraf. 1992. *El Niño: Historical and Paleoclimatic Aspects of the Southern Oscillation*. Cambridge University Press.

Dieppois, B., A. Capotondi, B. Pohl, K. P. Chun, P.-A. Monerie, and J. Eden. 2021. "Enso Diversity Shows Robust Decadal Variations That Must Be Captured for Accurate Future Projections." *Communications Earth & Environment* 2, no. 1: 212.

Dolman, A. M., T. Kunz, J. Groeneveld, and T. Laepple. 2021. "A Spectral Approach to Estimating the Timescale-Dependent Uncertainty of Paleoclimate Records – Part 2: Application and Interpretation." *Climate of the Past* 17, no. 2: 825–841. https://doi.org/10.5194/cp-17-825-2021.

Dunbar, R. B. 2000. "Clues From Corals." *Nature* 407, no. 6807: 956–959.

Emile-Geay, J., K. M. Cobb, M. Carré, et al. 2015. "Links Between Tropical Pacific Seasonal, Interannual and Orbital Variability During the Holocene." *Nature Geoscience* 9: 1–8.

Emile-Geay, J., K. M. Cobb, J. E. Cole, M. Elliot, and F. Zhu. 2020. "Past ENSO Variability: Reconstructions, Models and Implications." In *El Niño Southern Oscillation in a Changing Climate*, 87–118. Wiley. https://doi.org/10.1002/9781119548164.ch5.

Emile-Geay, J., K. M. Cobb, M. E. Mann, and A. T. Wittenberg. 2013a. "Estimating Central Equatorial Pacific SST Variability Over the Past Millennium. Part II: Reconstructions and Implications." *Journal of Climate* 26, no. 7: 2329–2352.

Emile-Geay, J., K. M. Cobb, M. E. Mann, and A. T. Wittenberg. 2013b. "Estimating Central Equatorial Pacific SST Variability Over the Past Millennium. Part I: Methodology and Validation." *Journal of Climate* 26, no. 7: 2302–2328.

Emile-Geay, J., and M. Tingley. 2015. "Inferring Climate Variability From Nonlinear Proxies: Application to Palaeo-ENSO Studies." *Climate of the Past* 12, no. 1: 31–50. https://doi.org/10.5194/cp-12-31-2016.

England, M. H., S. McGregor, P. Spence, et al. 2014. "Recent Intensification of Wind-Driven Circulation in the Pacific and the Ongoing Warming Hiatus." *Nature Climate Change* 4, no. 3: 222–227.

Evans, M. N., and R. G. Fairbanks. 1999. "The Thermal Oceanographic Signal of El Nino Reconstructed From a Kiritimati Island Coral." *Journal of Geophysical Research* 104, no. C6: 13409–13421.

Evans, M. N., A. Kaplan, and M. Cane. 1998. "Optimal Sites for Coral-Based Reconstruction of Global Sea Surface Temperature." *Paleoceanography* 13, no. 5: 502–516. https://doi.org/10.1029/98pa02132.

Evans, M. N., A. Kaplan, and M. Cane. 2000. "Intercomparison of Coral Oxygen Isotope Data and Historical Sea Surface Temperature (SST): Potential for Coral-Based SST Field Reconstructions." *Paleoceanography* 15, no. 5: 551–563.

Evans, M. N., A. Kaplan, and M. A. Cane. 2002. "Pacific Sea Surface Temperature Field Reconstruction From Coral δ18O Data Using Reduced Space Objective Analysis." *Paleoceanography* 17, no. 1: 7–7-13. https://doi.org/10.1029/2000pa000590.

Falster, G., B. Konecky, S. Coats, and S. Stevenson. 2023. "Forced Changes in the Pacific Walker Circulation Over the Past Millennium." *Nature* 622, no. 7981: 93–100. https://doi.org/10.1038/s41586-023-06447-0.

Fedorov, A. V., S. Hu, A. T. Wittenberg, A. F. Levine, and C. Deser. 2020. "Enso Low-Frequency Modulation and Mean State Interactions." In *El Niño Southern Oscillation in a Changing Climate*, 173–198. Wiley.

Frauen, C., D. Dommenget, N. Tyrrell, M. Rezny, and S. Wales. 2014. "Analysis of the Nonlinearity of El Niño–Southern Oscillation Teleconnections*." *Journal of Climate* 27, no. 16: 6225–6244. https://doi.org/10.1175/jcli-d-13-00757.1.

Fredriksen, H., J. Berner, A. C. Subramanian, and A. Capotondi. 2020. "How Does El Niño–Southern Oscillation Change Under Global Warming—A First Look at CMIP6." *Geophysical Research Letters* 47, no. 22: e2020GL090640. https://doi.org/10.1029/2020gl090640.

Freund, M. B., J. R. Brown, B. J. Henley, D. J. Karoly, and J. N. Brown. 2020. "Warming Patterns Affect El Niño Diversity in CMIP5 and CMIP6 Models." *Journal of Climate* 33, no. 19: 8237–8260. https://doi.org/10.1175/jcli-d-19-0890.1.

Freund, M. B., J. R. Brown, A. G. Marshall, et al. 2024. "Interannual ENSO Diversity, Transitions, and Projected Changes in Observations and Climate Models." *Environmental Research Letters* 19, no. 11: 114005. https://doi.org/10.1088/1748-9326/ad78db.

Freund, M. B., B. J. Henley, D. J. Karoly, H. V. McGregor, N. J. Abram, and D. Dommenget. 2019. "Higher Frequency of Central Pacific El Niño Events in Recent Decades Relative to Past Centuries." *Nature Geoscience* 12, no. 6: 450–455.

Garcia-Herrera, R., D. Barriopedro, E. Hernández, et al. 2008. "A Chronology of El Niño Events From Primary Documentary Sources in Northern Peru." *Journal of Climate* 21, no. 9: 1948–1962.

Gergis, J., K. Braganza, A. Fowler, S. Mooney, and J. Risbey. 2006. "Reconstructing El Niño–Southern Oscillation (Enso) From High-Resolution Palaeoarchives." *Journal of Quaternary Science* 21, no. 7: 707–722.

Gergis, J. L., and A. M. Fowler. 2005. "Classification of Synchronous Oceanic and Atmospheric El Niño-Southern Oscillation (ENSO) Events for Palaeoclimate Reconstruction." *International Journal of Climatology* 25, no. 12: 1541–1565.

Gergis, J. L., and A. M. Fowler. 2009. "A History of Enso Events Since Ad 1525: Implications for Future Climate Change." *Climatic Change* 92, no. 3: 343–387.

Glantz, M. H. 1996. *Currents of Change: El-Niño's Impact on Climate and Society*. Cambrige University Press.

Grothe, P. R., K. M. Cobb, G. Liguori, et al. 2020. "Enhanced El Niño–Southern Oscillation Variability in Recent Decades." *Geophysical Research Letters* 47, no. 7: e2019GL083906.

Guilyardi, E., A. Capotondi, M. Lengaigne, S. Thual, and A. T. Wittenberg. 2020. "Enso Modeling: History, Progress, and Challenges." In *El Niño Southern Oscillation in a Changing Climate*, 199–226. Wiley.

Hadley, G. 1735. "Concerning the Cause of the General Trade-Winds: By Geo. Hadley, Esq; F. R. S." *Philosophical Transactions of the Royal Society of London* 39: 58–62.

Hakim, G. J., J. Emile-Geay, E. J. Steig, et al. 2016. "The Last Millennium Climate Reanalysis Project: Framework and First Results." *Journal of Geophysical Research: Atmospheres* 121, no. 12: 6745–6764.

Ham, Y.-G., J.-S. Kug, J.-Y. Park, and F.-F. Jin. 2013. "Sea Surface Temperature in the North Tropical Atlantic as a Trigger for El Niño/Southern Oscillation Events." *Nature Geoscience* 6, no. 2: 112–116. https://doi.org/10.1038/ngeo1686.

Handler, P. 1984. "Possible Association of Stratospheric Aerosols and El Nino Type." *Geophysical Research Letters* 11: 1121–1124.

Hendon, H. H., E. Lim, G. Wang, O. Alves, and D. Hudson. 2009. "Prospects for Predicting Two Flavors of El Niño." *Geophysical Research Letters* 36, no. 19: L19713. https://doi.org/10.1029/2009gl040100.

Hendon, H. H., and M. L. Salby. 1994. "The Life Cycle of the Madden–Julian Oscillation." *Journal of the Atmospheric Sciences* 51, no. 15: 2225–2237.

Henley, B. J. 2017. "Pacific Decadal Climate Variability: Indices, Patterns and Tropical-Extratropical Interactions." *Global and Planetary Change* 155: 42–55.

Hope, P., B. J. Henley, J. Gergis, J. Brown, and H. Ye. 2017. "Time-Varying Spectral Characteristics of Enso Over the Last Millennium." *Climate Dynamics* 49: 1705–1727.

Hou, M., and Y. Tang. 2022. "Recent Progress in Simulating Two Types of ENSO From CMIP5 to CMIP6." *Frontiers in Marine Science* 9: 986780. https://doi.org/10.3389/fmars.2022.986780.

Hu, Z.-Z., M. J. McPhaden, A. Kumar, J.-Y. Yu, and N. C. Johnson. 2020. "Uncoupled El Niño Warming." *Geophysical Research Letters* 47, no. 7: e2020GL087621.

Jiang, L., K. Yu, S. Tao, Y. Li, and S. Wang. 2023. "Abrupt Increase in ENSO Variability at 700 CE Triggered by Solar Activity." *Journal of Geophysical Research. Oceans* 128, no. 1: e2022JC019278. https://doi.org/10.1029/2022jc019278.

Jiang, X., Á. F. Adames, D. Kim, et al. 2020. "Fifty Years of Research on the Madden-Julian Oscillation: Recent Progress, Challenges, and Perspectives." *Journal of Geophysical Research. Atmospheres* 125, no. 17: e2019JD030911.

Johnson, N. C. 2013. "How Many ENSO Flavors Can we Distinguish?" *Journal of Climate* 26, no. 13: 4816–4827.

Jungclaus, J. H., E. Bard, M. Baroni, et al. 2017. "The pmip4 Contribution to cmip6—Part 3: The Last Millennium, Scientific Objective, and Experimental Design for the pmip4 *past1000* Simulations." *Geoscientific Model Development* 10, no. 11: 4005–4033. https://doi.org/10.5194/gmd-10-4005-2017.

Kahya, E., and J. A. Dracup. 1993. "Us Streamflow Patterns in Relation to the El Niño/Southern Oscillation." *Water Resources Research* 29, no. 8: 2491–2503.

Kao, H.-Y., and J.-Y. Yu. 2009. "Contrasting Eastern-Pacific and Central-Pacific Types of ENSO." *Journal of Climate* 22, no. 3: 615–632. https://doi.org/10.1175/2008jcli2309.1.

Karamperidou, C., and P. N. DiNezio. 2022. "Holocene Hydroclimatic Variability in the Tropical Pacific Explained by Changing ENSO Diversity." *Nature Communications* 13, no. 1: 7244. https://doi.org/10.1038/s41467-022-34880-8.

Karamperidou, C., P. N. D. Nezio, A. Timmermann, F. Jin, and K. M. Cobb. 2015. "The Response of ENSO Flavors to Mid-Holocene Climate: Implications for Proxy Interpretation." *Paleoceanography* 30, no. 5: 527–547. https://doi.org/10.1002/2014pa002742.

Kaufman, D., N. McKay, C. Routson, et al. 2020. "Holocene Global Mean Surface Temperature, a Multi-Method Reconstruction Approach." *Scientific Data* 7, no. 1: 201. https://doi.org/10.1038/s41597-020-0530-7.

Kim, H.-R., K.-J. Ha, S. Moon, H. Oh, and S. Sharma. 2020. "Impact of the Indo-Pacific Warm Pool on the Hadley, Walker, and Monsoon Circulations." *Atmosphere* 11, no. 10: 1030. https://doi.org/10.3390/atmos11101030.

Kim, S. T., and J. Yu. 2012. "The Two Types of ENSO in CMIP5 Models." *Geophysical Research Letters* 39, no. 11: L11704. https://doi.org/10.1029/2012gl052006.

Klockmann, M., U. von Toussaint, and E. Zorita. 2022. "Towards Variance-Conserving Reconstructions of Climate Indices With Gaussian Process Regression in an Embedding Space." *Geoscientific Model Development Discussions* 2022: 1–33.

Kosaka, Y., and S.-P. Xie. 2013. "Recent Global-Warming Hiatus Tied to Equatorial Pacific Surface Cooling." *Nature* 501, no. 7467: 403–407.

Kug, J.-S., F.-F. Jin, and S.-I. An. 2009. "Two Types of El Niño Events: Cold Tongue El El Niño and Warm Pool El El Niño." *Journal of Climate* 22, no. 6: 1499–1515.

Kug, J.-S., and I.-S. Kang. 2006. "Interactive Feedback Between ENSO and the Indian Ocean." *Journal of Climate* 19, no. 9: 1784–1801. https://doi.org/10.1175/jcli3660.1.

Larkin, N. K., and D. E. Harrison. 2005. "Global Seasonal Temperature and Precipitation Anomalies During El Niño Autumn and Winter." *Geophysical Research Letters* 32, no. 16: L16705.

Lawman, A. E., P. N. D. Nezio, J. W. Partin, S. G. Dee, K. Thirumalai, and T. M. Quinn. 2022. "Unraveling Forced Responses of Extreme El Niño Variability Over the Holocene." *Science Advances* 8, no. 9: eabm4313. https://doi.org/10.1126/sciadv.abm4313.

Lewis, S. C., and A. N. LeGrande. 2015. "Stability of Enso and Its Tropical Pacific Teleconnections Over the Last Millennium." *Climate of the Past* 11, no. 10: 1347–1360.

L'Heureux, M. L., D. S. Harnos, E. Becker, et al. 2024. "How Well Do Seasonal Climate Anomalies Match Expected El Niño–Southern Oscillation (ENSO) Impacts?" *Bulletin of the American Meteorological Society* 105, no. 8: E1542–E1551. https://doi.org/10.1175/bams-d-23-0252.1.

Li, J., S. Xie, E. Cook, et al. 2011. "Interdecadal Modulation of El Niño Amplitude During the Past Millennium." *Nature Climate Change* 1, no. 2: 114–118.

Li, J., S.-P. Xie, E. R. Cook, et al. 2013. "El Niño Modulations Over the Past Seven Centuries." *Nature Climate Change* 3, no. 9: 822–826.

Li, S., L. Wu, Y. Yang, et al. 2020. "The Pacific Decadal Oscillation Less Predictable Under Greenhouse Warming." *Nature Climate Change* 10, no. 1: 30–34. https://doi.org/10.1038/s41558-019-0663-x.

Lieber, R., J. Brown, A. King, and M. Freund. 2024. "Historical and Future Asymmetry of ENSO Teleconnections With Extremes." *Journal of Climate* 37, no. 22: 5909–5924. https://doi.org/10.1175/jcli-d-23-0619.1.

Liguori, G., and E. D. Lorenzo. 2018. "Meridional Modes and Increasing Pacific Decadal Variability Under Anthropogenic Forcing." *Geophysical Research Letters* 45, no. 2: 983–991. https://doi.org/10.1002/2017gl076548.

Lin, J., and T. Qian. 2019. "A New Picture of the Global Impacts of El Nino-Southern Oscillation." *Scientific Reports* 9, no. 1: 17543.

Liu, Y., W. Cai, X. Lin, Z. Li, and Y. Zhang. 2023. "Nonlinear El Niño Impacts on the Global Economy Under Climate Change." *Nature Communications* 14, no. 1: 5887.

Liu, Y., K. M. Cobb, H. Song, et al. 2017. "Recent Enhancement of Central Pacific El Niño Variability Relative to Last Eight Centuries." *Nature Communications* 8, no. 1: 15386. https://doi.org/10.1038/ncomms15386.

Liu, Y., W. Man, T. Zhou, and M. Zuo. 2024. "Global Multiproxy Enso Reconstruction Over the Past Millennium." *Journal of Geophysical Research: Atmospheres* 129, no. 10: e2023JD040491.

Liu, Z., Z. Lu, X. Wen, B. L. Otto-Bliesner, A. Timmermann, and K. M. Cobb. 2014. "Evolution and Forcing Mechanisms of El Niño Over the Past 21,000 Years." *Nature* 515, no. 7528: 550–553. https://doi.org/10.1038/nature13963.

Lu, Z., Z. Liu, J. Zhu, and K. M. Cobb. 2018. "A Review of Paleo El Niño-Southern Oscillation." *Atmosphere* 9, no. 4: 130.

Maher, N., T. P. Tabarin, and S. Milinski. 2022. "Combining Machine Learning and Smiles to Classify, Better Understand, and Project Changes in Enso Events." *Earth System Dynamics* 13, no. 3: 1289–1304.

Maher, N., R. C. J. Wills, P. DiNezio, et al. 2023. "The Future of the El Niño–Southern Oscillation: Using Large Ensembles to Illuminate Time-Varying Responses and Inter-Model Differences." *Earth System Dynamics* 14, no. 2: 413–431. https://doi.org/10.5194/esd-14-413-2023.

Mann, M. E. 2002. "The Value of Multiple Proxies." *Science* 297, no. 5586: 1481–1482. https://doi.org/10.1126/science.1074318.

Mann, M. E., R. S. Bradley, and M. K. Hughes. 2000. *Long-Term Variability in the El Nino Southern Oscillation and Associated Teleconnections*. Cambridge University Press.

Marathe, S., K. Ashok, P. Swapna, and T. P. Sabin. 2015. "Revisiting El Niño Modokis." *Climate Dynamics* 45, no. 11–12: 3527–3545. https://doi.org/10.1007/s00382-015-2555-8.

Marshall, J., and R. A. Plumb. 2016. *Atmosphere, Ocean and Climate Dynamics: An Introductory Text*. Vol. 21. Academic Press.

Martín-Gómez, V., B. Rodríguez-Fonseca, I. Polo, and M. Martín-Rey. 2024. "Observed Global Mean State Changes Modulating the Collective Influence of the Tropical Atlantic and Indian Oceans on ENSO." *Journal of Climate* 37, no. 15: 3869–3886. https://doi.org/10.1175/jcli-d-23-0450.1.

McBride, J. L., and N. Nicholls. 1983. "Seasonal Relationships Between Australian Rainfall and the Southern Oscillation." *Monthly Weather Review* 111, no. 10: 1998–2004.

McGregor, H. V., and N. J. Abram. 2008. "Images of Diagenetic Textures in Porites Corals From Papua New Guinea and Indonesia." *Geochemistry, Geophysics, Geosystems* 9, no. 10: Q10013. https://doi.org/10.1029/2008gc002093.

McGregor, S., A. Gallant, and P. v. Rensch. 2024. "Quantifying ENSOs Impact on Australia's Regional Monthly Rainfall Risk." *Geophysical Research Letters* 51, no. 6: e2023GL106298. https://doi.org/10.1029/2023gl106298.

McGregor, S., M. Khodri, N. Maher, M. Ohba, F. S. R. Pausata, and S. Stevenson. 2020. "The Effect of Strong Volcanic Eruptions on ENSO." In *Geophysical Monograph Series*, 267–287. American Geophysical Union (AGU). https://doi.org/10.1002/9781119548164.ch12.

McGregor, S., A. Timmermann, M. H. England, O. E. Timm, and A. T. Wittenberg. 2013. "Inferred Changes in El Niño–Southern Oscillation Variance Over the Past Six Centuries." *Climate of the Past* 9, no. 5: 2269–2284. https://doi.org/10.5194/cp-9-2269-2013.

McGregor, S., A. Timmermann, and O. Timm. 2010. "A Unified Proxy for ENSO and PDO Variability Since 1650." *Climate of the Past* 6, no. 1: 1–17.

McPhaden, M. J., T. Lee, S. Fournier, and M. A. Balmaseda. 2020. "ENSO Observations." In *El Niño Southern Oscillation in a Changing Climate*, vol. 3, 39–63. American Geophysical Union.

McPhaden, M. J., A. Santoso, and W. Cai. 2020. *Introduction to El Niño Southern Oscillation in a Changing Climate*, 1–19. Wiley. https://doi.org/10.1002/9781119548164.ch1.

Moss, M. E., C. P. Pearson, and A. I. McKerchar. 1994. "The Southern Oscillation Index as a Predictor of the Probability of Low Streamflows in New Zealand." *Water Resources Research* 30, no. 10: 2717–2723.

Moy, C. M., G. O. Seltzer, D. T. Rodbell, and D. M. Anderson. 2002. "Variability of El Niño/Southern Oscillation Activity at Millennial Timescales During the Holocene Epoch." *Nature* 420, no. 6912: 162–165. https://doi.org/10.1038/nature01194.

Murtagh, F., and P. Legendre. 2014. "Ward's Hierarchical Agglomerative Clustering Method: Which Algorithms Implement Ward's Criterion?" *Journal of Classification* 31, no. 3: 274–295. https://doi.org/10.1007/s00357-014-9161-z.

Newman, M., M. A. Alexander, T. R. Ault, et al. 2016. "The Pacific Decadal Oscillation, Revisited." *Journal of Climate* 29, no. 12: 4399–4427. https://doi.org/10.1175/jcli-d-15-0508.1.

Newman, M., S. Shin, and M. A. Alexander. 2011. "Natural Variation in ENSO Flavors." *Geophysical Research Letters* 38, no. 14: L14705. https://doi.org/10.1029/2011gl047658.

Okumura, Y. M., T. Sun, and X. Wu. 2017. "Asymmetric Modulation of El Niño and La Niña and the Linkage to Tropical Pacific Decadal Variability." *Journal of Climate* 30, no. 12: 4705–4733. https://doi.org/10.1175/jcli-d-16-0680.1.

Oliver, J. 2005. *The Encyclopedia of World Climatology (Encyclopedia of Earth Sciences Series)*, 54. Springer.

Ortlieb, L. 2000. "The Documented Historical Record of El Niño Events in Peru: An Update of the Quinn Record (Sixteenth through Nineteenth Centuries)." In *El Niño and the Southern Oscillation: Multiscale Variability and Global and Regional Impacts*, edited by H. F. Diaz and V. Markgraf, 207–296. Cambridge University Press.

Otto-Bliesner, B. L., E. C. Brady, J. Fasullo, et al. 2016. "Climate Variability and Change Since 850 Ce: An Ensemble Approach With the Community Earth System Model." *Bulletin of the American Meteorological Society* 97, no. 5: 735–754. https://doi.org/10.1175/BAMS-D-14-00233.1.

Peel, M., T. McMahon, B. Finlayson, and F. Watson. 2001. "Identification and Explanation of Continental Differences in the Variability of Annual Runoff." *Journal of Hydrology* 250, no. 1–4: 224–240.

Penland, C., D. Z. Sun, A. Capotondi, and D. J. Vimont. 2013. "A Brief Introduction to El Niño and La Niña." In *Climate Dynamics: Why Does Climate Vary?* 53–64. American Geophysical Union (AGU).

Philander, S. G. 1990. "El Niño, La Niña, and the Southern Oscillation." *Science* 46: 904–905. https://doi.org/10.1126/science.248.4957.904.

Phillips, J., M. Cane, and C. Rosenzweig. 1998. "Enso, Seasonal Rainfall Patterns and Simulated Maize Yield Variability in Zimbabwe." *Agricultural and Forest Meteorology* 90, no. 1–2: 39–50.

Piechota, T. C., and J. A. Dracup. 1996. "Drought and Regional Hydrologic Variation in the United States: Associations With the El Niño-Southern Oscillation." *Water Resources Research* 32, no. 5: 1359–1373.

Piechota, T. C., J. A. Dracup, and R. G. Fovell. 1997. "Western Us Streamflow and Atmospheric Circulation Patterns During El Niño-Southern Oscillation." *Journal of Hydrology* 201, no. 1–4: 249–271.

Planton, Y. Y., E. Guilyardi, A. T. Wittenberg, et al. 2021. "Evaluating Climate Models With the Clivar 2020 Enso Metrics Package." *Bulletin of the American Meteorological Society* 102, no. 2: E193–E217.

Potgieter, A. B., G. L. Hammer, and D. Butler. 2002. "Spatial and Temporal Patterns in Australian Wheat Yield and Their Relationship With Enso." *Australian Journal of Agricultural Research* 53, no. 1: 77–89.

Power, S., T. Casey, C. Folland, A. Colman, and V. Mehta. 1999. "Inter-Decadal Modulation of the Impact of ENSO on Australia." *Climate Dynamics* 15: 319–324.

Power, S., M. Lengaigne, A. Capotondi, et al. 2021. "Decadal Climate Variability in the Tropical Pacific: Characteristics, Causes, Predictability, and Prospects." *Science* 374, no. 6563: eaay9165. https://doi.org/10.1126/science.aay9165.

Quinn, N., and D. Mayolo. 1987. "El Niño Occurrences Over the Past Four and a Half Centuries." *Journal of Geophysical Research* 92, no. C13: 14449.

Quinn, W., and W. H. Quinn. 1993. "The Large-Scale Enso Event, the El Niño and Other Important Regional Features." *Bulletin de l'Institut français d'études andines* 22, no. 1: 13–34.

Quinn, W. H. 1992. "A Study of Southern Oscillation-Related Climatic Activity for A.D. 622–1900 Incorporating Nile River Flood Data." In *El Niño: Historical and Paleoclimatic Aspects of the Southern Oscillation*, edited by H. F. Diaz and V. Markgraf, 119–149. Cambridge University Press.

Quinn, W. H., and W. V. Burt. 1970. "Prediction of Abnormally Heavy Precipitation Over the Equatorial Pacific Dry Zone." *Journal of Applied Meteorology* 9, no. 1: 20–28.

Quinn, W. H., and V. Neal. 1992. "The Historical Record of El Niño Events." In *Climate Since AD 1500*, 623–648. Routledge.

Quinn, W. H., D. O. Zopf, K. S. Short, and R. K. Yang. 1978. "Historical Trends and Statistics of the Southern Oscillation, El Niño, and Indonesian Droughts." *Fishery Bulletin* 76, no. 3: 663–678.

Rajagopalan, B., E. Cook, U. Lall, and B. K. Ray. 2000. "Spatiotemporal Variability of Enso and Sst Teleconnections to Summer Drought Over the United States During the Twentieth Century." *Journal of Climate* 13, no. 24: 4244–4255.

Rasmusson, E. M., and T. H. Carpenter. 1982. "Variation in Tropical Sea Surface Temperature and Surface Wind Fields Associated With the Southern Oscillation/El Niño." *Monthly Weather Review* 110: 354.

Rayner, N. A., D. E. Parker, and E. B. Horton. 2003. "Global Analyses of Sea Surface Temperature, Sea Ice, and Night Marine Air Temperature Since the Late Nineteenth Century." *Journal of Geophysical Research* 108, no. D14: 4407.

Ren, H.-L., W. Zhang, T. Lian, R. Xie, and M. Hayashi. 2022. "Editorial: ENSO Nonlinearity and Complexity: Features, Mechanisms, Impacts and Prediction." *Frontiers in Earth Science* 10: 967362. https://doi.org/10.3389/feart.2022.967362.

Rimmington, G. M., and N. Nicholls. 1993. "Forecasting Wheat Yields in Australia With the Southern Oscillation Index." *Australian Journal of Agricultural Research* 44, no. 4: 625–632.

Ropelewski, C. F., and M. S. Halpert. 1987. "Global and Regional Scale Precipitation Patterns Associated With the El Niño/Southern Oscillation." *Monthly Weather Review* 115, no. 8: 1606–1626.

Ropelewski, C. F., and P. D. Jones. 1987. "An Extension of the Tahiti-Darwin Southern Oscillation Index." *Monthly Weather Review* 115, no. 9: 2161–2165.

Sanchez, S. C., D. J. Amaya, A. J. Miller, S.-P. Xie, and C. D. Charles. 2019. "The Pacific Meridional Mode Over the Last Millennium." *Climate Dynamics* 53, no. 5–6: 3547–3560. https://doi.org/10.1007/s00382-019-04740-1.

Santoso, A., M. J. McPhaden, and W. Cai. 2017. "The Defining Characteristics of ENSO Extremes and the Strong 2015/16 El Niño." *Reviews of Geophysics* 55, no. 4: 1079–1129.

Sazib, N., L. E. Mladenova, and J. D. Bolten. 2020. "Assessing the Impact of Enso on Agriculture Over Africa Using Earth Observation Data." *Frontiers in Sustainable Food Systems* 4: 509914.

Schlör, J., A. Capotondi, and B. Goswami. 2023. "A Multi-Modal Representation of El-Niño Southern Oscillation Diversity." https://doi.org/10.5194/egusphere-egu23-2136.

Schlör, J., F. Strnad, A. Capotondi, and B. Goswami. 2024. "Contribution of El Niño Southern Oscillation (Enso) Diversity to Low-Frequency Changes in Enso Variance." *Geophysical Research Letters* 51, no. 14: e2024GL109179. https://doi.org/10.1029/2024gl109179.

Schneider, T. 2001. "Analysis of Incomplete Climate Data: Estimation of Mean Values and Covariance Matrices and Imputation of Missing Values." *Journal of Climate* 14, no. 5: 853–871. https://doi.org/10.1175/1520-0442(2001)014<0853:aoicde>2.0.co;2.

Schott, F. A., S. Xie, and J. P. McCreary. 2009. "Indian Ocean Circulation and Climate Variability." *Reviews of Geophysics* 47, no. 1: RG1002. https://doi.org/10.1029/2007rg000245.

Schroeter, N., J. L. Toney, S. Lauterbach, et al. 2020. "How to Deal With Multi-Proxy Data for Paleoenvironmental Reconstructions: Applications to a Holocene Lake Sediment Record From the Tian Shan, Central Asia." *Frontiers in Earth Science* 8: 353. https://doi.org/10.3389/feart.2020.00353.

Sengupta, A., A. D. King, and J. R. Brown. 2025. "Do CMIP6 Models Capture Seasonal and Regional Differences in the Asymmetry of ENSO-Precipitation Teleconnections?" *Journal of Geophysical Research: Atmospheres* 130, no. 2: e2024JD041031. https://doi.org/10.1029/2024jd041031.

Shimizu, M. H., and T. Ambrizzi. 2016. "Mjo Influence on Enso Effects in Precipitation and Temperature Over South America." *Theoretical and Applied Climatology* 124: 291–301.

Sippel, S., E. C. Kent, N. Meinshausen, et al. 2024. "Early-Twentieth-Century Cold Bias in Ocean Surface Temperature Observations." *Nature* 635, no. 8039: 618–624. https://doi.org/10.1038/s41586-024-08230-1.

Smerdon, J. E. 2012. "Climate Models as a Test Bed for Climate Reconstruction Methods: Pseudoproxy Experiments." *WIREs Climate Change* 3, no. 1: 63–77. https://doi.org/10.1002/wcc.149.

Stahle, D. W., and M. K. Cleaveland. 1993. "Southern Oscillation Extremes Reconstructed From Tree Rings of the Sierra Madre Occidental and Southern Great Plains." *Journal of Climate* 6, no. 1: 129–140.

Stahle, D. W., R. D. D'Arrigo, P. J. Krusic, et al. 1998. "Experimental Dendroclimatic Reconstruction of the Southern Oscillation." *Bulletin of the American Meteorological Society* 79, no. 10: 2137–2152.

Stevenson, S., A. Capotondi, J. Fasullo, and B. Otto-Bliesner. 2019. "Forced Changes to Twentieth Century Enso Diversity in a Last Millennium Context." *Climate Dynamics* 52: 7359–7374.

Stevenson, S., H. V. McGregor, S. J. Phipps, and B. Fox-Kemper. 2013. "Quantifying Errors in Coral-Based ENSO Estimates: Toward Improved Forward Modeling of $\delta$18O." *Paleoceanography* 28, no. 4: 633–649.

Stevenson, S., B. Otto-Bliesner, J. Fasullo, and E. Brady. 2016. ""El Niño like" hydroclimate responses to last millennium volcanic eruptions." *Journal of Climate* 29, no. 8: 2907–2921. https://doi.org/10.1175/JCLI-D-15-0239.1.

Stevenson, S., B. L. Otto-Bliesner, E. C. Brady, et al. 2019. "Volcanic Eruption Signatures in the Isotope-Enabled Last Millennium Ensemble." *Paleoceanography and Paleoclimatology* 34, no. 8: 1534–1552. https://doi.org/10.1029/2019PA003625.

Stevenson, S., J. T. Overpeck, J. Fasullo, et al. 2018. "Climate Variability, Volcanic Forcing, and Last Millennium Hydroclimate Extremes." *Journal of Climate* 31, no. 11: 4309–4327. https://doi.org/10.1175/JCLI-D-17-0407.1.

Sun, D.-Z., and F. Bryan. 2013. *Climate Dynamics: Why Does Climate Vary?* American Geophysical Union (AGU).

Tapper, N., and L. Hurry. 1993. *Australia's Weather Patterns: An Introductory Guide*. Dellasta.

Tardif, R., G. J. Hakim, W. A. Perkins, et al. 2019. "Last Millennium Reanalysis With an Expanded Proxy Database and Seasonal Proxy Modeling." *Climate of the Past* 15, no. 4: 1251–1273.

Taschetto, A. S., A. S. Gupta, N. C. Jourdain, A. Santoso, C. C. Ummenhofer, and M. H. England. 2014. "Cold Tongue and Warm Pool ENSO Events in CMIP5: Mean State and Future Projections." *Journal of Climate* 27, no. 8: 2861–2885. https://doi.org/10.1175/jcli-d-13-00437.1.

Taschetto, A. S., C. C. Ummenhofer, M. F. Stuecker, et al. 2020. "Enso Atmospheric Teleconnections." In *El Niño Southern Oscillation in a Changing Climate*, 309–335. Wiley.

Thirumalai, K., P. N. DiNezio, J. W. Partin, D. Liu, K. Costa, and A. Jacobel. 2024. "Future Increase in Extreme El Niño Supported by Past Glacial Changes." *Nature* 634, no. 8033: 374–380. https://doi.org/10.1038/s41586-024-07984-y.

Tierney, J. E., N. J. Abram, K. J. Anchukaitis, et al. 2015. "Tropical Sea Surface Temperatures for the Past Four Centuries Reconstructed From Coral Archives." *Paleoceanography* 30, no. 3: 226–252.

Timmermann, A., S.-I. An, J.-S. Kug, et al. 2018. "El Niño–Southern Oscillation Complexity." *Nature* 559, no. 7715: 535–545. https://doi.org/10.1038/s41586-018-0252-6.

Torbenson, M., D. Stahle, I. Howard, et al. 2019. "Multidecadal Modulation of the Enso Teleconnection to Precipitation and Tree Growth Over Subtropical North America." *Paleoceanography and Paleoclimatology* 34, no. 5: 886–900.

Trenberth, K. E. 2020. "ENSO in the Global Climate System." *El Niño Southern Oscillation in a Changing Climate. Geophysical Monograph Series* 2020: 21–37.

Trenberth, K. E., and D. P. Stepaniak. 2001. "Indices of El Niño Evolution." *Journal of Climate* 14, no. 8: 1697–1701.

Troup, A. 1965. "The 'Southern Oscillation'." *Quarterly Journal of the Royal Meteorological Society* 91, no. 390: 490–506.

Tudhope, A. W., C. P. Chilcott, M. T. McCulloch, et al. 2001. "Variability in the El Niño-Southern Oscillation Through a Glacial-Interglacial Cycle." *Science* 291, no. 5508: 1511–1517. https://doi.org/10.1126/science.1057969.

Vincent, D. G. 1994. "The South-Pacific Convergence Zone (Spcz)—A Review." *Monthly Weather Review* 122, no. 9: 1949–1970.

von Storch, H., E. Zorita, J. M. Jones, Y. Dimitriev, F. González-Rouco, and S. F. B. Tett. 2004. "Reconstructing Past Climate From Noisy Data." *Science* 306, no. 5696: 679–682. https://doi.org/10.1126/science.1096109.

Wang, G.-G., H. Cheng, Y. Zhang, and H. Yu. 2023. "Enso Analysis and Prediction Using Deep Learning: A Review." *Neurocomputing* 520: 216–229.

Ward, P. J., S. Eisner, M. Flörke, M. D. Dettinger, and M. Kummu. 2014. "Annual Flood Sensitivities to El Niño–Southern Oscillation at the Global Scale." *Hydrology and Earth System Sciences* 18, no. 1: 47–66. https://doi.org/10.5194/hess-18-47-2014.

Ward, P. J., B. Jongman, M. Kummu, M. D. Dettinger, F. C. Sperna Weiland, and H. C. Winsemius. 2014. "Strong Influence of El Niño Southern Oscillation on Flood Risk Around the World." *Proceedings of the National Academy of Sciences* 111, no. 44: 15659–15664.

Whetton, P., and I. Rutherfurd. 1994. "Historical Enso Teleconnections in the Eastern Hemisphere." *Climatic Change* 28, no. 3: 221–253.

Wiedermann, M., J. F. Siegmund, J. F. Donges, and R. V. Donner. 2021. "Differential Imprints of Distinct ENSO Flavors in Global Patterns of Very Low and High Seasonal Precipitation." *Frontiers in Climate* 3: 618548. https://doi.org/10.3389/fclim.2021.618548.

Wilcox, P. S., M. Mudelsee, C. Spötl, and R. L. Edwards. 2023. "Solar Forcing of ENSO on Century Timescales." *Geophysical Research Letters* 50, no. 20: e2023GL105201. https://doi.org/10.1029/2023gl105201.

Wills, R. C., T. Schneider, J. M. Wallace, D. S. Battisti, and D. L. Hartmann. 2018. "Disentangling Global Warming, Multidecadal Variability, and El Niño in Pacific Temperatures." *Geophysical Research Letters* 45, no. 5: 2487–2496.

Wilson, R., E. Cook, R. D'Arrigo, et al. 2010. "Reconstructing Enso: The Influence of Method, Proxy Data, Climate Forcing and Teleconnections." *Journal of Quaternary Science* 25, no. 1: 62–78.

Wittenberg, A. T. 2009. "Are Historical Records Sufficient to Constrain ENSO Simulations?" *Geophysical Research Letters* 36, no. 12: L12702. https://doi.org/10.1029/2009gl038710.

Wolter, K., and M. S. Timlin. 1998. "Measuring the Strength of Enso Events: How Does 1997/98 Rank?" *Weather* 53, no. 9: 315–324.

Wright, P. B. 1985. "The Southern Oscillation: An Ocean–Atmosphere Feedback System?" *Bulletin of the American Meteorological Society* 66, no. 4: 398–412.

Wu, L., F. He, and Z. Liu. 2005. "Coupled Ocean-Atmosphere Response to North Tropical Atlantic SST: Tropical Atlantic Dipole and ENSO." *Geophysical Research Letters* 32, no. 21: L21712. https://doi.org/10.1029/2005gl024222.

Wyman, D. A., J. L. Conroy, and C. Karamperidou. 2020. "The Tropical Pacific Enso–Mean State Relationship in Climate Models Over the Last Millennium." *Journal of Climate* 33, no. 17: 7539–7551. https://doi.org/10.1175/JCLI-D-19-0673.1.

Wyrtki, K. 1975. "El Niño—The Dynamic Response of the Equatorial Pacific Oceanto Atmospheric Forcing." *Journal of Physical Oceanography* 5, no. 4: 572–584. https://doi.org/10.1175/1520-0485(1975)005<0572:entdro>2.0.co;2.

Wyrtki, K. 1985. "Water Displacements in the Pacific and the Genesis of El Niño Cycles." *Journal of Geophysical Research: Oceans* 90, no. C4: 7129–7132.

Yasunaka, S., and K. Hanawa. 2010. "Intercomparison of Historical Sea Surface Temperature Datasets." *International Journal of Climatology* 31, no. 7: 1056–1073.

Yeh, S.-W., J.-S. Kug, and S.-I. An. 2014. "Recent Progress on Two Types of El Niño: Observations, Dynamics, and Future Changes." *Asia-Pacific Journal of Atmospheric Sciences* 50, no. 1: 69–81. https://doi.org/10.1007/s13143-014-0028-3.

Yeh, S.-W., J.-S. Kug, B. Dewitte, M.-H. Kwon, B. P. Kirtman, and F.-F. Jin. 2009. "El Niño in a Changing Climate." *Nature* 461, no. 7263: 511–514. https://doi.org/10.1038/nature08316.

Yeo, S.-R., S.-W. Yeh, K.-Y. Kim, and W. Kim. 2017. "The Role of Low-Frequency Variation in the Manifestation of Warming Trend and Enso Amplitude." *Climate Dynamics* 49, no. 4: 1197–1213.

Yu, J., and S. T. Kim. 2013. "Identifying the Types of Major El Niño Events Since 1870." *International Journal of Climatology* 33, no. 8: 2105–2112. https://doi.org/10.1002/joc.3575.

Yuan, C., and T. Yamagata. 2015. "Impacts of Iod, Enso and Enso Modoki on the Australian Winter Wheat Yields in Recent Decades." *Scientific Reports* 5, no. 1: 17252.

Yuan, Y., and H. Yan. 2013. "Different Types of La Niña Events and Different Responses of the Tropical Atmosphere." *Chinese Science Bulletin* 58: 406–415.

Zhang, H., A. Clement, and P. D. Nezio. 2013. "The South Pacific Meridional Mode: A Mechanism for ENSO-Like Variability." *Journal of Climate* 27, no. 2: 130917124100006. https://doi.org/10.1175/jcli-d-13-00082.1.

Zhang, Z., S. Wagner, M. Klockmann, and E. Zorita. 2022. "Evaluation of Statistical Climate Reconstruction Methods Based on Pseudoproxy Experiments Using Linear and Machine-Learning Methods." *Climate of the Past* 18, no. 12: 2643–2668.

Zhu, F., J. Emile-Geay, K. J. Anchukaitis, et al. 2022. "A Re-Appraisal of the ENSO Response to Volcanism With Paleoclimate Data Assimilation." *Nature Communications* 13, no. 1: 747. https://doi.org/10.1038/s41467-022-28210-1.